Supporting Information

A novel porphyrin MOF catalyst for efficient conversion of CO_2 with propargyl amine

Contents:

1. Experimental Section.

1.1 Materials and methods

All substrates were used as received from commercial suppliers, unless otherwise stated. Chemicals were purchased from Sigma-Aldrich, Chempur, TCI, or Alfa Aesar.

^{1}HNMR data were collected on a Varian INOVA-600 MHz, Bruker Avance III 400 MHz spectrometer at ambient temperature. Fourier transform infrared (FT-IR) spectra were recorded as KBr pellets on JASCO FT/IR-430 spectrometer. Powder XRD diffractograms were obtained on a Rigaku D/Max-2400 X-ray diffractometer with a sealed Cu tube (λ = 1.54178 Å). IR spectra were recorded as KBr pellets on a NEXUS instrument. Thermogravimetric analyses (TGA) were performed at a ramp rate of 10 °C/min in a nitrogen flow with an SDTQ600 instrument. The solid UV−vis spectra were recorded on a Hitachi U-4100 UV−vis−NIR spectrophotometer. Liquid UV-vis spectra were recorded on a TU-1900 spectrophotometer. X-ray photoelectron spectroscopy (XPS) signals were collected on a Thermo ESCALAB Xi^{+} spectrometer.

Dye uptake experiment ： The Cu- TCPP(Fe) crystals were immersed in the methanol saturated solution of malachite green, measure the UV absorption intensity of the liquid at regular intervals and calculate the dye adsorption amount based on changes in absorbance. After 24 hours, the crystals were thoroughly washed with methanol until the solution was clarified. Add the dye loaded Cu-TCPP(Fe) to the methanol solution and measure the UV absorption intensity of the liquid at regular intervals, calculate dye release based on changes in absorbance.

1.2 Syntheses and methods

Synthesis procedure of ligand Fe-TCPP

The ligands [5,10,15,20-Tetrakis(4-carboxyphenyl) porphyrinato] Fe^{III} Chloride (Fe-TCPP) were synthesized according to the previously reported literatures. [S1, S2]

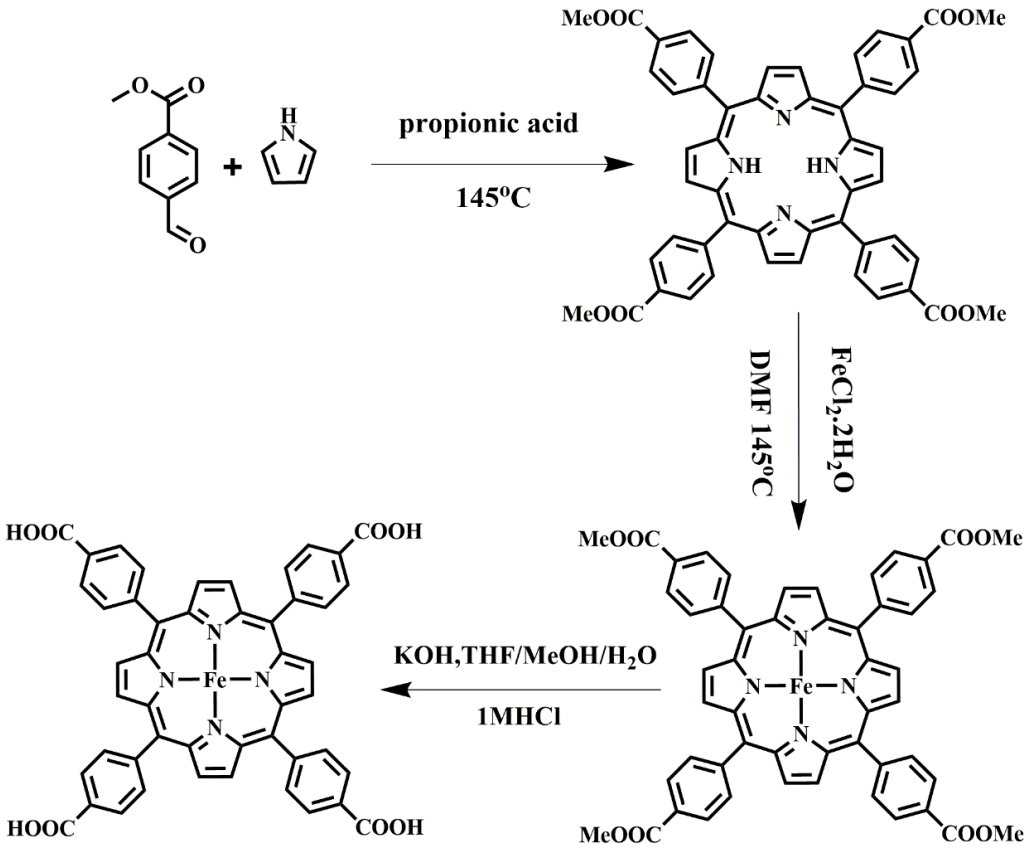

Scheme S1. Synthetic procedure for tetrakis(4-carboxyphenyl) porphyrin (Fe-TCPP).

(1) Synthesis of compound TCPPMe

Firstly, dissolve methyl p-formylbenzoate (7g, 42.6mmol) in propionic acid(200ml), and then add pyrrole (3g, 44.7mmol) dropwise to the above solution. Reflux the mixed solution at 145 ℃ overnight After the reaction mixture was reduced to room temperature, the purple crystal products were obtained by suction filtration and washed with methanol and water. Yield: 33%

(2) Synthesis of ferric chloride porphyrin complex Fe-TCPPMe.

TCPPMe (1.5 g, 1.77 mmol) and $FeCl_2$•$4H_2O$ (5 g, 25.6 mmol) were put into DMF (200 mL) and then heated to reflux for 12 h. The obtained precipitate was obtained by

suction filtration and washed twice with water. The remaining solid was dissolved in chloroform and purified using solvent extraction (1 M HCl extraction for 3 times and water extraction for 2 times). And the quantitative dark brown crystals were obtained by spin evaporation. Yield: 70%

(3) Synthesis of Fe-TCPP.

Fe-TCPPMe (1.5 g,1.67mmol) was stirred with a mixture of THF (50 mL) and MeOH (50mL), followed by the addition of KOH solution, in which 5.2 g KOH was dissolved in 50 mL water. The mixture was in a reflux state (85℃) for 12 h. After the reaction mixture was reduced to room temperature, THF and MeOH were evaporated. Additional water was added to the resulting aqueous phase, and the mixture was heated until the solid was completely dissolved. The resulting homogeneous solution was then acidified with 1 $mol \cdot L^{-1}$ HCl until the precipitate was no longer formed. The brown solid was obtained by filtering with water and drying in a vacuum. The solid was collected by filtration, washed with water, and dried in vacuum. Yield: 85%.

The synthetic procedure of Cu−TCPP(Fe).

$CuCl_2 .2H_2O$ (30 mg, 0.176 mmol, 14.7 equiv), Fe-TCPP (10 mg, 0.012 mmol, 1.0 equiv), and trifluoroacetic acid (0.3 mL) were ultrasonically dissolved in 3.5 mL of DMF/acetonitrile/H_2O ($v_1/v_2/v_3$ = 4:2:1) in a 7 mL Pyrex vial. The resultant solution was heated to 125 °C for 2 days in Teflon-lined autoclave and subsequently cooled to room temperature with a rate of 0.1 K/min. Bright red crystals materials (pure phase Cu-TCPP(Fe)) were obtained via filtration and washed with DMF (3 × 10 mL) and acetone (2 × 10 mL). The crystals were covered with acetone (5 mL), allowed to stand for 24 h, and collected by filtration. Yield: 85% based on Cu.

The synthetic procedure of Cu−TCPP(Co).

The synthesis of Co-TCPP is similar to that of Fe-TCPP. $CuCl_2$.$2H_2O$ (30 mg, 0.176 mmol, 14.7 equiv), Co-TCPP (10 mg, 0.012 mmol, 1.0 equiv), and trifluoroacetic acid (0.2 mL) were ultrasonically dissolved in 3 mL of DMF/acetonitrile/H_2O ($v_1/v_2/v_3$ = 4:1:1) in a 7 mL Pyrex vial. The resultant solution was heated to 125 °C for 2 days in Teflon-lined autoclave and subsequently cooled to room temperature with a rate of 0.1 K/min. Obtain deep blue needle shaped crystals. The cleaning method is consistent with Cu-TCPP(Fe). Yield: 50% based on Cu

The synthetic procedure of Cu−TCPP(Ni).

The synthesis of Ni-TCPP is similar to that of Fe-TCPP. $CuCl_2$.$2H_2O$ (30 mg, 0.176 mmol, 14.7 equiv), Fe-TCPP (10 mg, 0.012 mmol, 1.0 equiv), and trifluoroacetic acid (0.05 mL) were ultrasonically dissolved in 3.25 mL of DMF/acetonitrile/H_2O ($v_1/v_2/v_3$ = 8:4:1) in a 7 mL Pyrex vial. The resultant solution was heated to 125 °C for 2 days in Teflon-lined autoclave and subsequently cooled to room temperature with a rate of 0.1 K/min. Obtain red needle shaped crystals. The cleaning method is consistent with Cu-TCPP(Fe). Yield: 90% based on Cu

2. Single Crystal X-ray Crystallography.

Single-Crystal Analysis. X-ray intensity data were carried out on a Bruker SMART APEX charge-coupled device-based diffractometer (Mo Kα radiation, λ 0.71073 Å) with the SAINT and SMART programs. The SAINT software was used in the data integration and reduction. Empirical absorption correction, which was applied to the collected reflection, worked with SADABS. SHELXTL was used to solve the structures

in direct methods, which was refined on F^2 by the full-matrix least-squares method with the program SHELXL-97.

In the structural refinement of Cu-TCPP(Fe), all of the non-hydrogen atoms were refined anisotropically. The hydrogen atoms within the ligand backbones were fixed geometrically at calculated distances and allowed to ride on the parent non-hydrogen atoms. The SQUEEZE subroutine in PLATON was used.

Table 1. Crystal data and structure refinements.

Compound	Cu-TCPP(Fe)
Empirical formula	$C_{48}H_{25}CuN_4O_9Fe$
Formula weight	921.11
Temperature/K	250.0
Crystal system	monoclinic
Space group	*Ia*
a/Å	8.1724(10)
b/Å	26.209(2)
c/Å	23.090(2)
α/°	90
β/°	91.734(6)
γ/°	90
Volume/Å^3	4943.4(8)
Z	4
ρ_{calc}g/cm^3	1.238
μ/mm^{-1}	0.777
F (000)	1872.0
Crystal size/mm^3	0.2×0.1×0.03
Radiation	MoKα (λ = 0.71073)
2 theta range for data collection/°	4.704 to 50.046
Index ranges	$-9 \le h \le 9$, $-31 \le k \le 27$, $-27 \le l \le 27$
Reflections collected	16161
Independent reflections	8062 [R_{int} = 0.1774, R_{sigma} = 0.1865]
Data/restraints/parameters	7560/1704/482
Goodness-of-fit on F^2	1.023
Final R indexes [$I>=2\sigma(I)$]	R_1 = 0.1352, wR_2 = 0.3214
Final R indexes [all data]	R_1 = 0.1972, wR_2 = 0.3778
Largest diff. peak/hole / e Å^{-3}	4.39/-1.09
CCDC number	2328973

3. Characterizations of Catalysts.

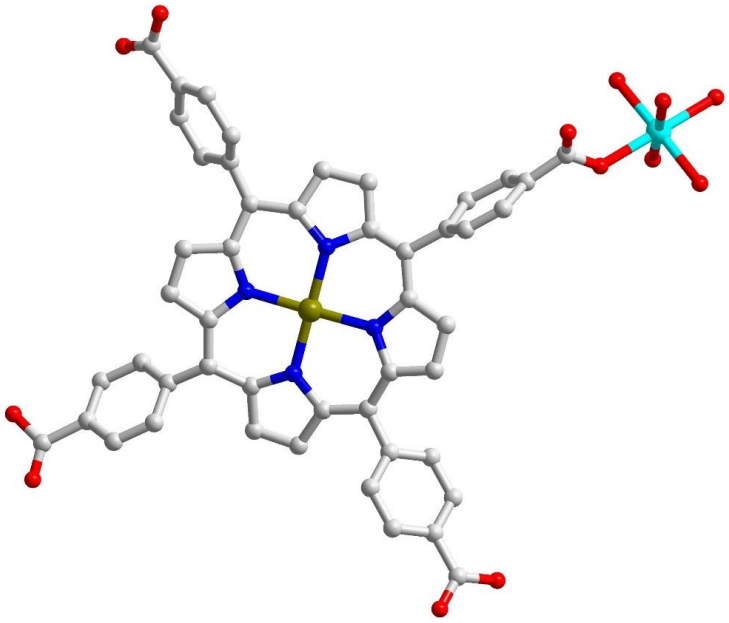

Figure S1. Single-crystal X-ray diffraction structure of Cu-TCPP(Fe) asymmetric unit. Iron = blackish green, Oxygen = red, Carbon = grey, Copper = cyan. Hydrogen atoms, solvent and anion are omitted for clarity.

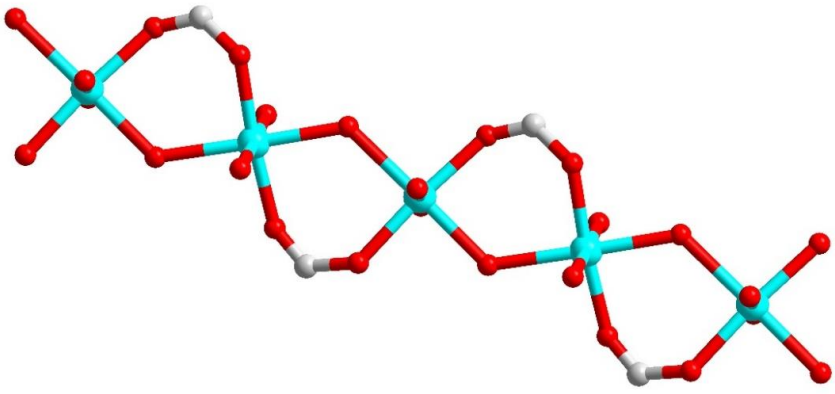

Figure S2. The coordinated environments and the polyhedral representation of one-dimensional Cu-O-Cu chain.

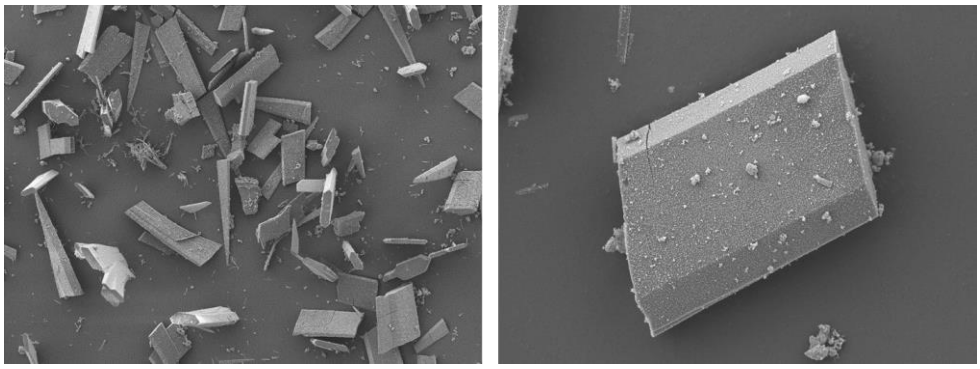

Figure S3. A magnified SEM image of the as-synthesized Cu-TCPP(Fe).

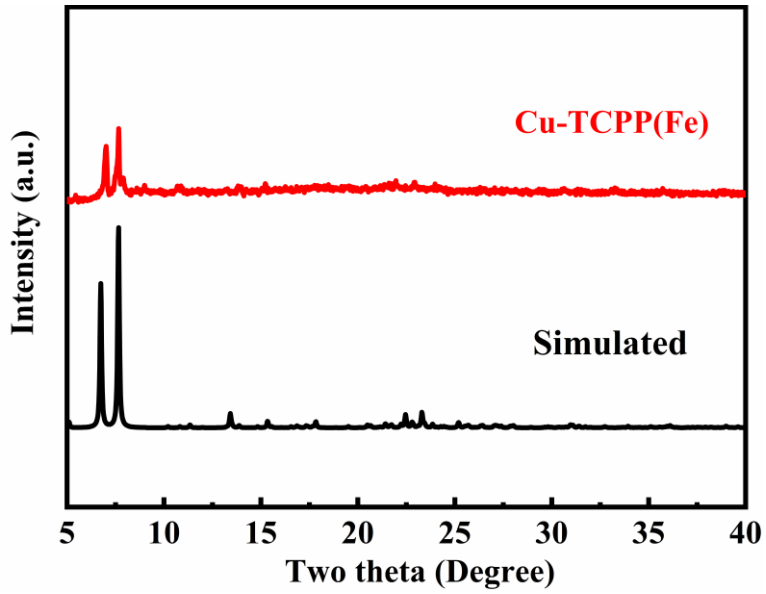

Figure S4. X-ray powder diffraction (XRD) patterns of freshly prepared Cu-TCPP(Fe) (red) and its simulated pattern based single-crystal data (black)

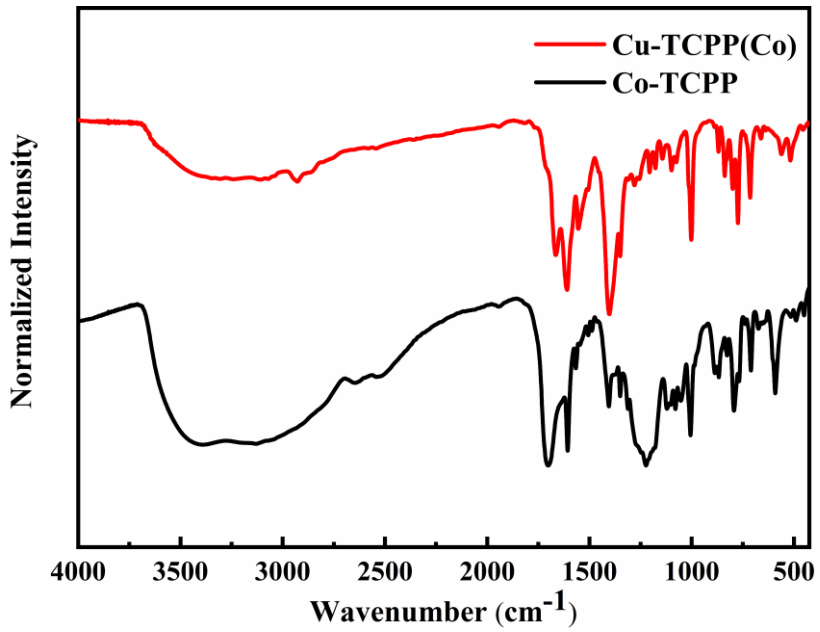

Figure S5. IR spectra of Cu-TCPP(Co) (red line) and ligand Co-TCPP (black line).

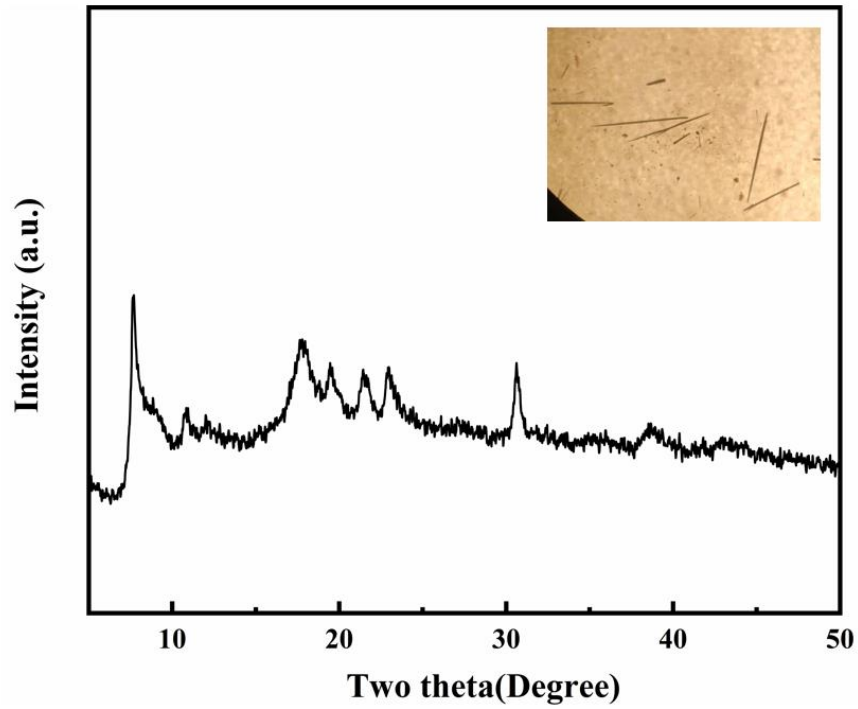

Figure S6. X-ray powder diffraction (XRD) patterns of Cu-TCPP(Co); insert (Microscopic crystal images).

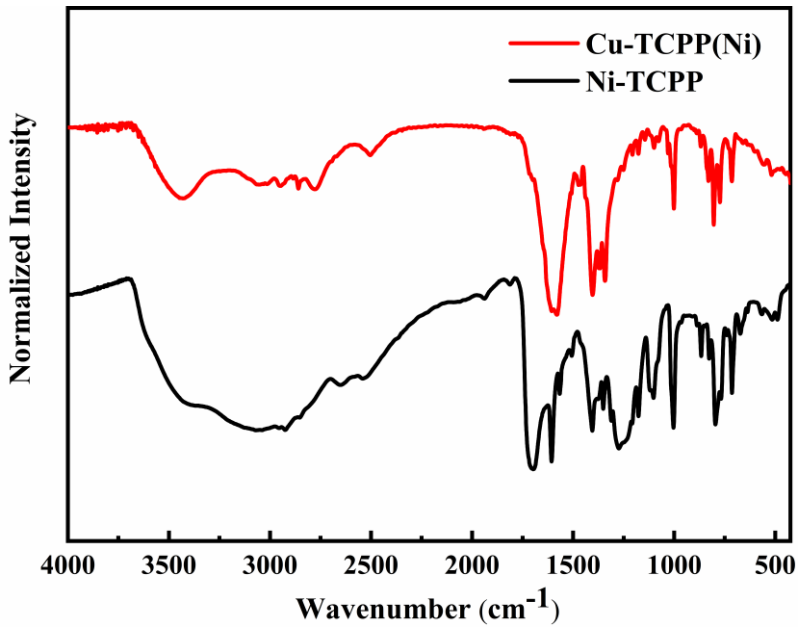

Figure S7. IR spectra of Cu-TCPP(Ni) (red line) and ligand Ni-TCPP (black line).

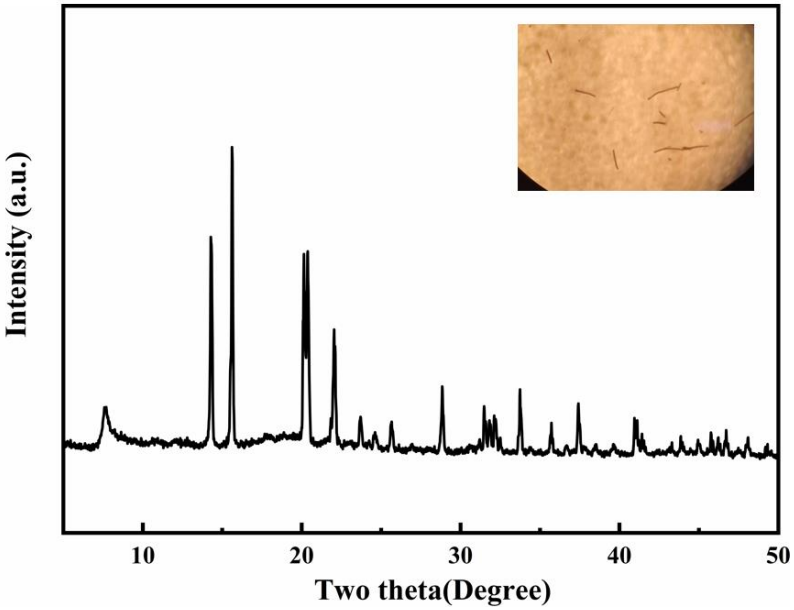

Figure S8. X-ray powder diffraction (XRD) patterns of Cu-TCPP(Ni); insert (Microscopic crystal images).

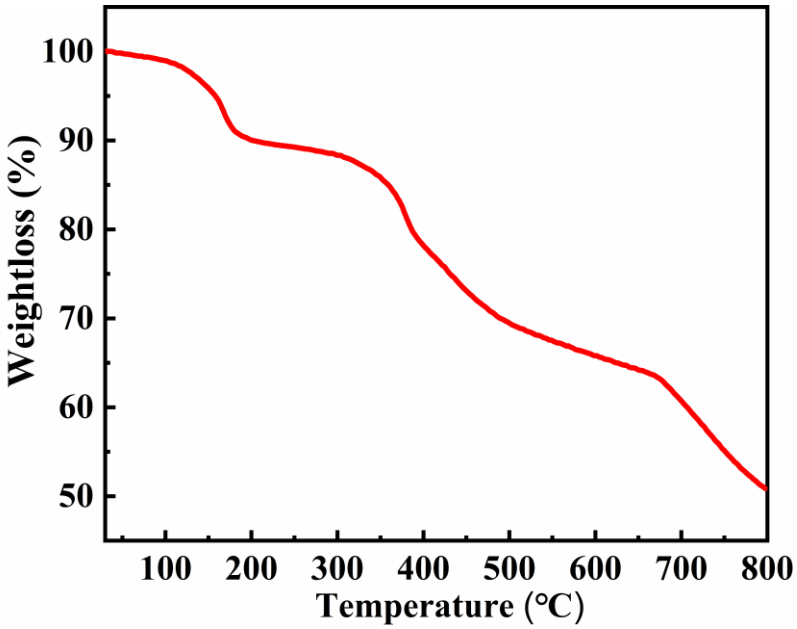

Figure S9. Thermogravimetric (TGA) figure of Cu-TCPP(Fe) with heating rates of 10℃ /min.

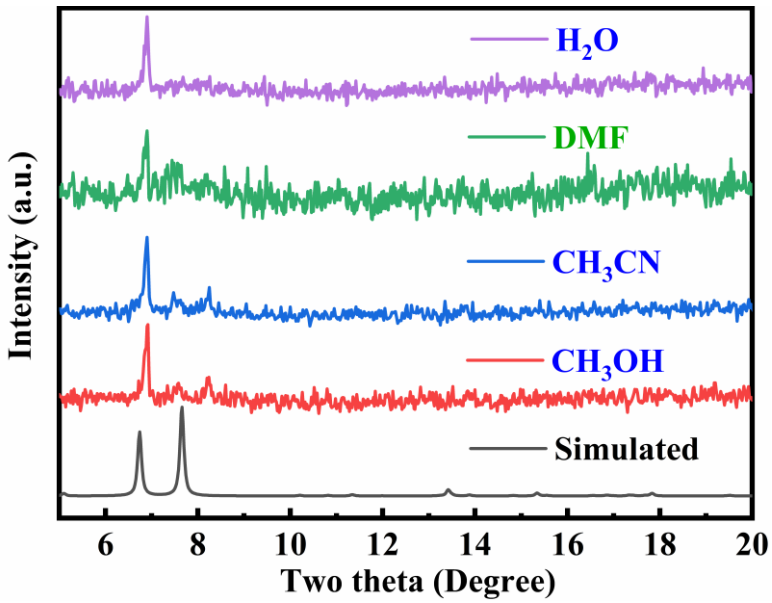

Figure S10. X-ray powder diffraction (XRD) patterns of Cu-TCPP(Fe) soaked in different solvents.

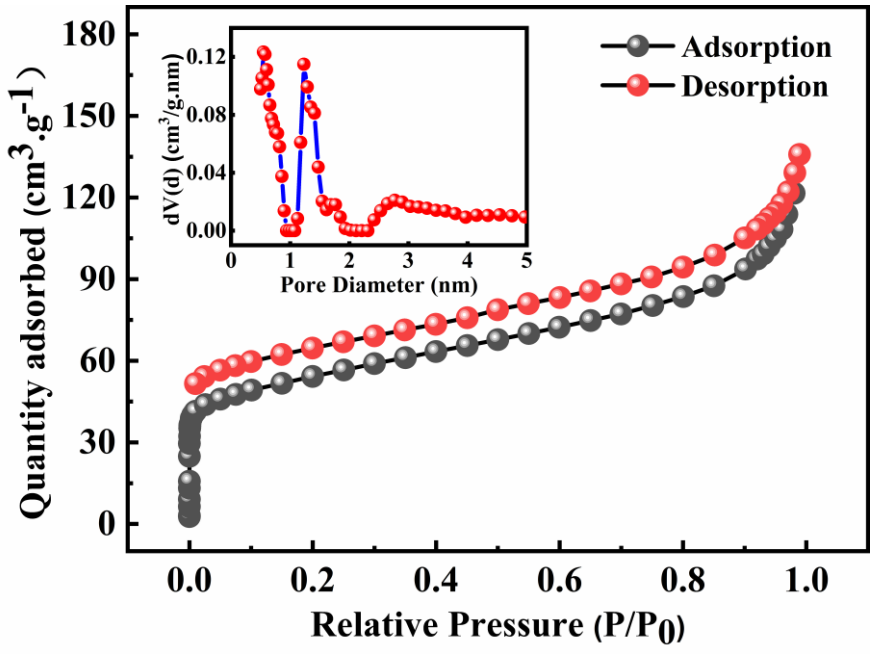

Figure S11. N_2 adsorption–desorption isotherms of Cu-TCPP(Fe). Insert is the pore size distribution of Cu-TCPP(Fe).

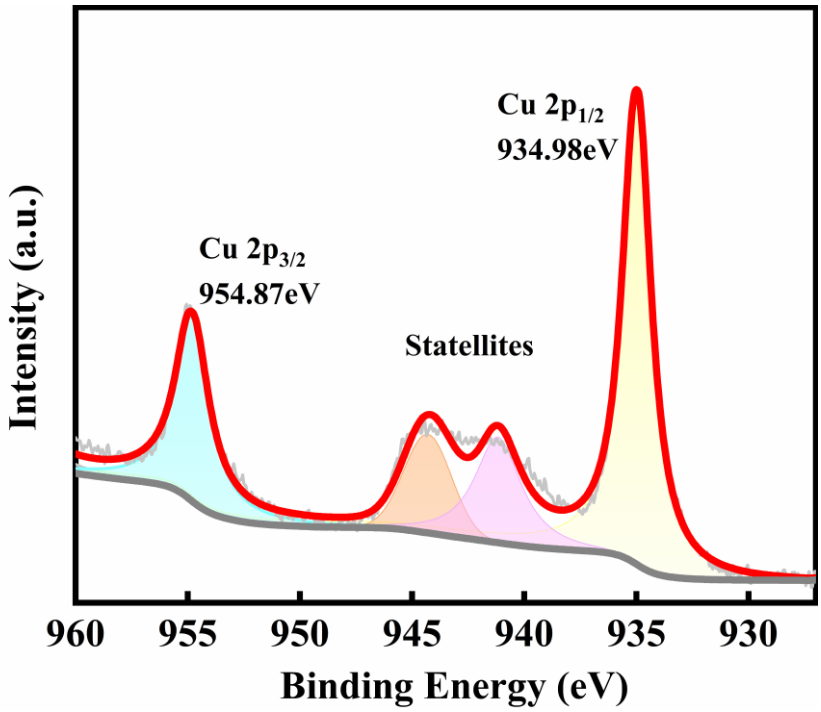

Figure S12. The XPS spectra of Cu^{II} ions in Cu-TCPP(Fe).

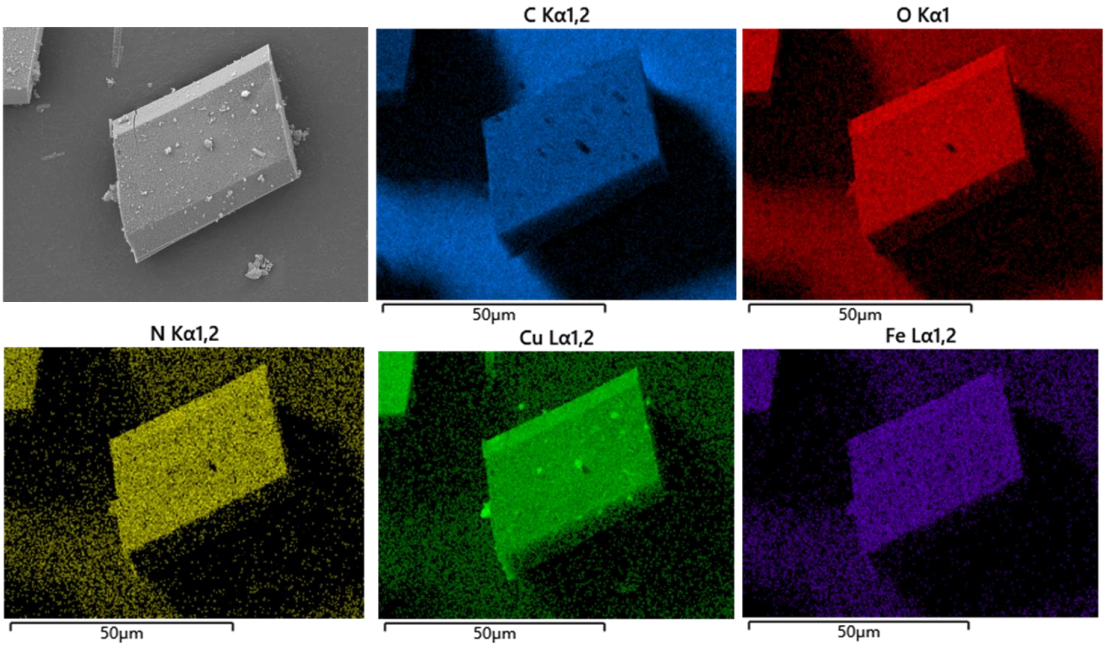

Figure S13. SEM and the EDS mapping images of Cu-TCPP(Fe).

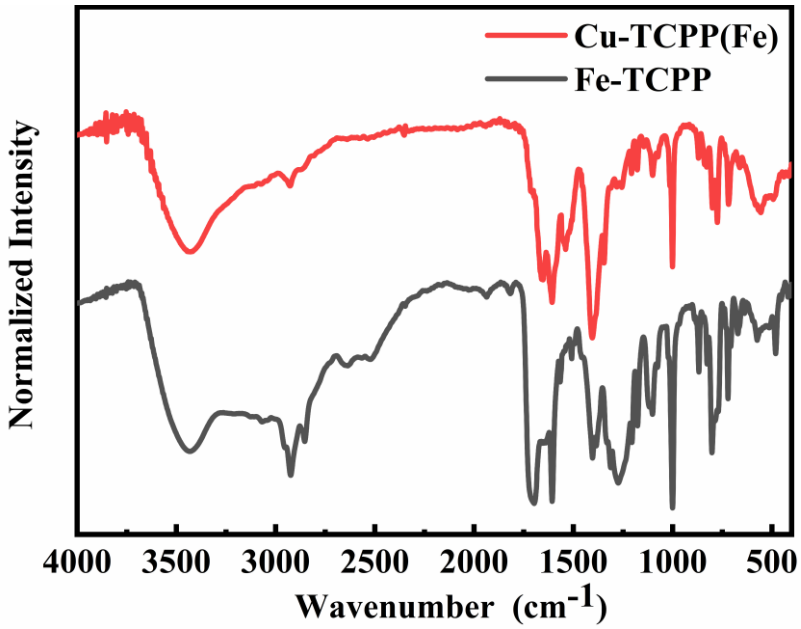

Figure S14. IR spectra of Cu-TCPP(Fe) (red line) and ligand Fe-TCPP (black line).

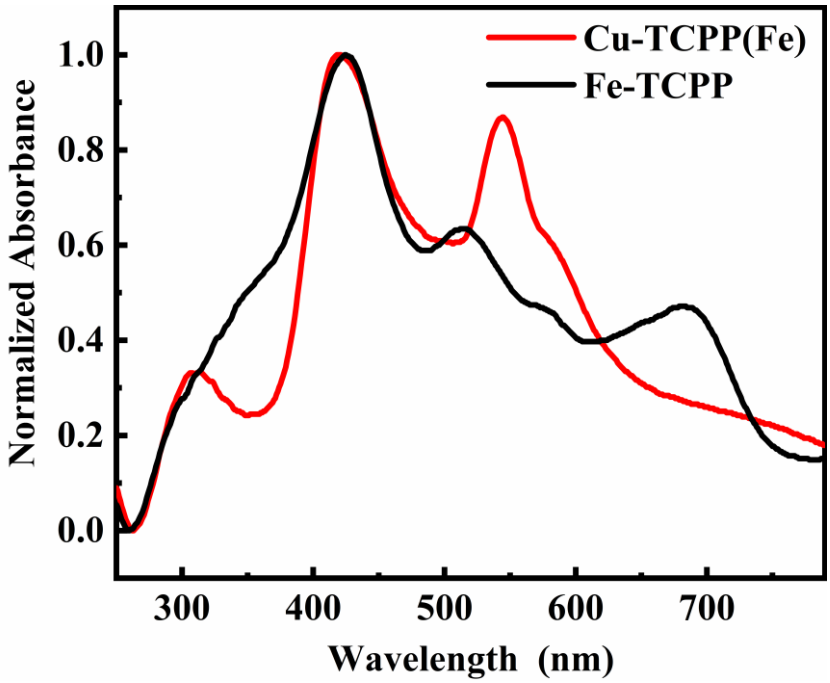

Figure S15. UV-vis absorption for ground Cu- TCPP(Fe) (red line) and Fe-TCPP powder (black line).

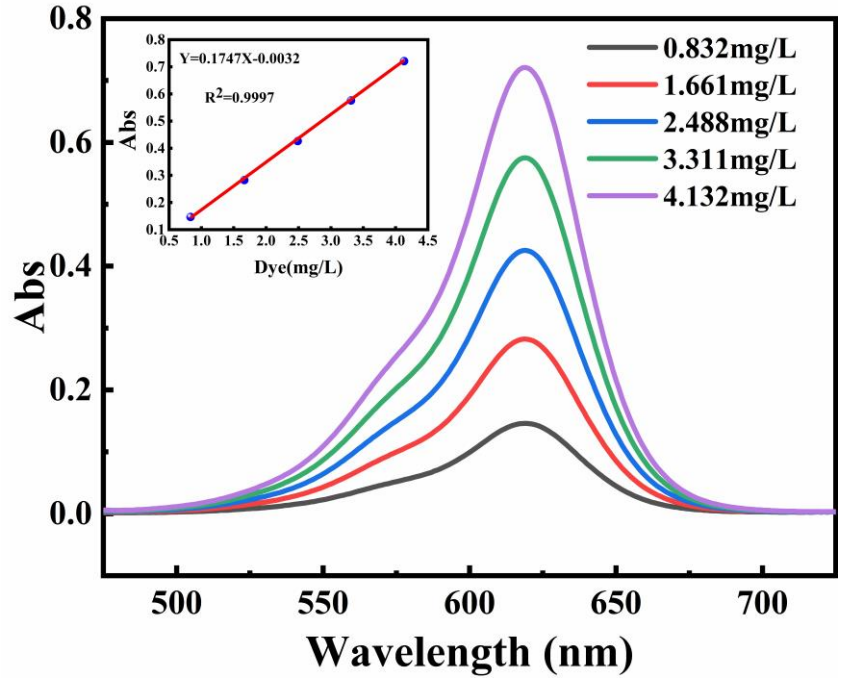

Figure S16. The UV-vis spectrum of different concentrations of malachite green dye. The standard linear relationship between the absorption and the concentration.

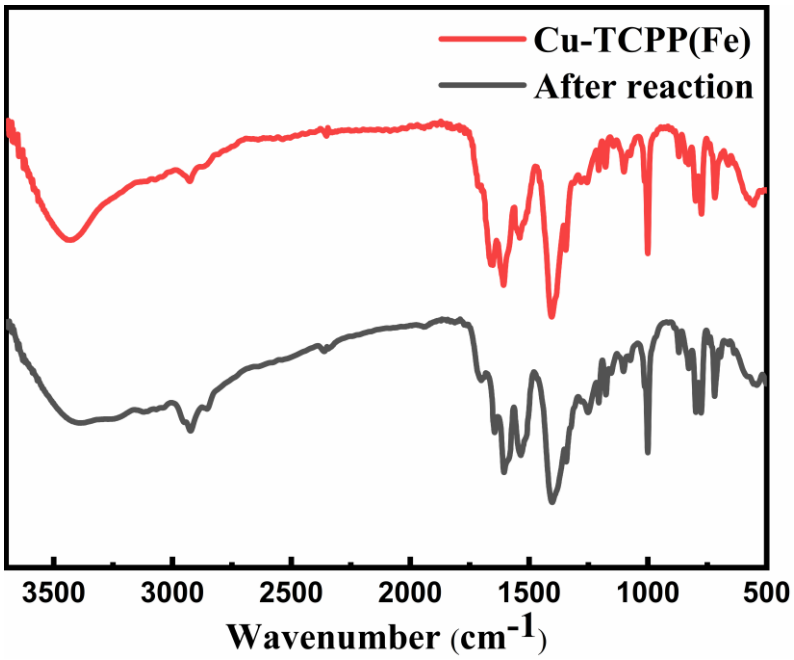

Figure S17. IR spectra of freshly prepared Cu-TCPP(Fe) (red) and Cu- TCPP(Fe) after reaction(black).

4. Catalysis Details

N-methylpropargylamine (1a): The substrate 1a was purchased from Energy Chemical and used without further purification.

N-(prop-2-yn-1-yl) butan-1-amine (2a) and N-(cyclohexylmethyl) prop-2-yn-1-amine (3a): The substrate 2a was prepared according to previous reference. [S3,S4]

Synthesis and Characterization of Propargylic Amines (4a-12a): One drop of acetic acid was added to the mixture of propargylamine (12mmol, 0.661g) and benzaldehyde (13mmol, 1.38g) in 20ml methanol. The solution was stirred at room temperature for 24 hours. Then, the mixture was cooled to 0°C, and $NaBH_4$ (18mmol, 0.68g) was added in portions. The mixture was allowed warmed to room temperature and stirred for 1h. The solution was evaporated to dryness and 100mL water was added. The aqueous phase was extracted with CH_2Cl_2 (50mL×2) and then the organic phase was extracted with 1M HCl (50mL×3). $NaHCO_3$ was added to neutralize the solution and the mixture was extracted with CH_2Cl_2 (50mL×2). The organic extracts were washed with brine (50mL) and dried ($MgSO_4$). The filtrate was concentrated under reduced pressure, andfurther purification via silica gel chromatography to afford the pure products. [S5]

N-Methylmaleimide (1a): ^{1}H NMR (400 MHz, MeCN-d3)) δ 3.32 (d, J = 2.5 Hz, 2H), 2.46 (t, J = 2.4 Hz, 1H), 2.37 (s, 3H), 1.83 (s, 1H).

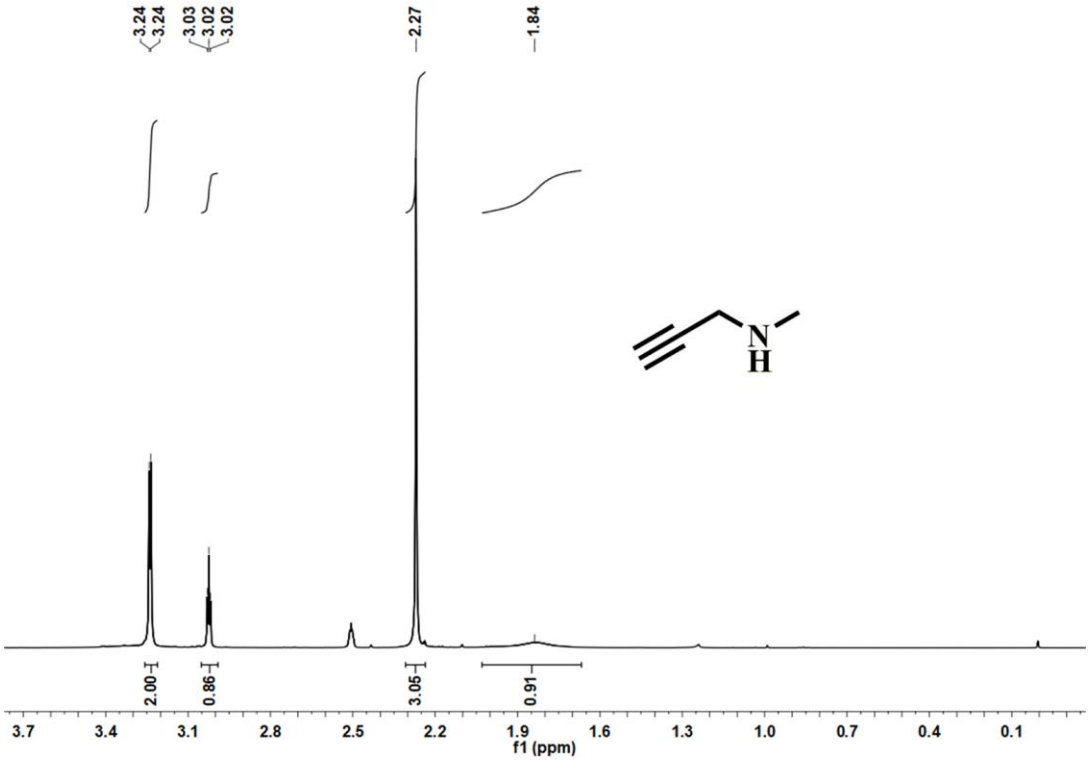

3-methyl-5-methyleneoxazolidin-2-one (1b): ^{1}H NMR (400 MHz, DMSO) δ 4.63 (q, *J* = 2.6 Hz, 1H), 4.35 (dd, *J* = 4.9, 2.3 Hz, 1H), 4.22 (t, *J* = 2.4 Hz, 2H), 2.80 (s, 3H).

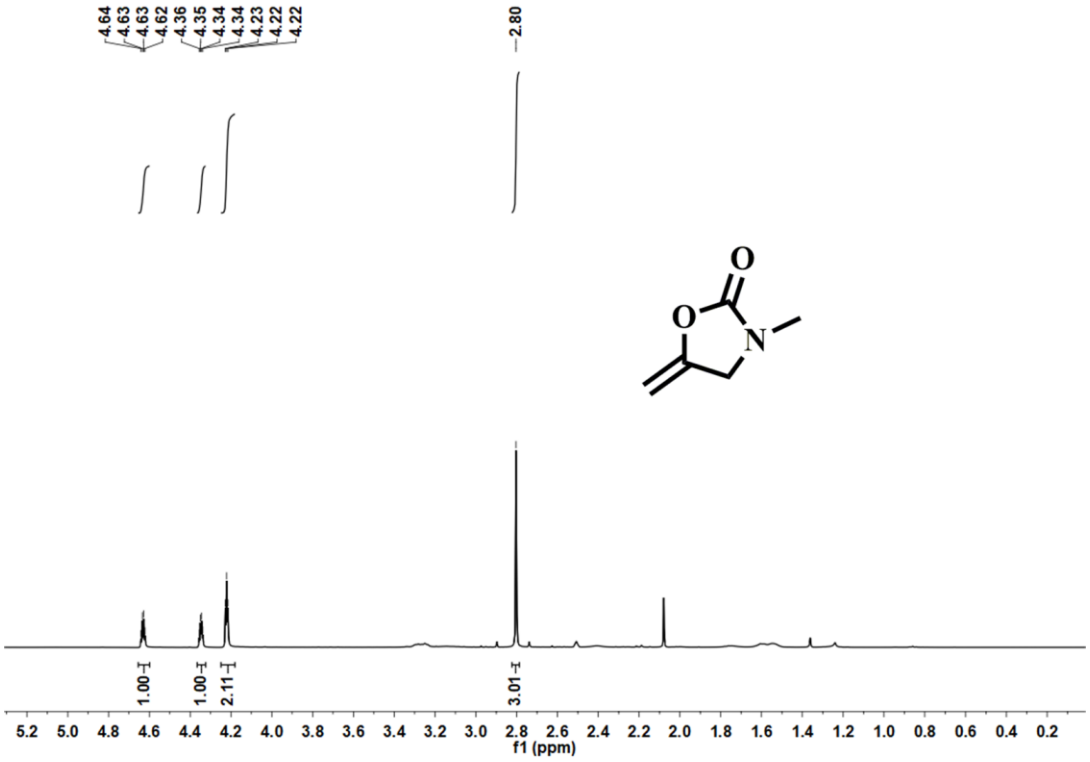

N-(prop-2-yn-1-yl) butan-1-amine (2a): ^{1}H NMR (400 MHz, Chloroform-d) δ 3.42 (d, J = 2.5 Hz, 2H), 2.68 (t, J = 7.1 Hz, 2H), 2.20 (t, J = 2.4 Hz, 1H), 1.47 (q, J = 7.6, 7.1 Hz, 2H), 1.40 – 1.34 (m, 2H), 1.34 – 1.24 (m, 1H), 0.91 (t, J = 7.3 Hz, 3H)

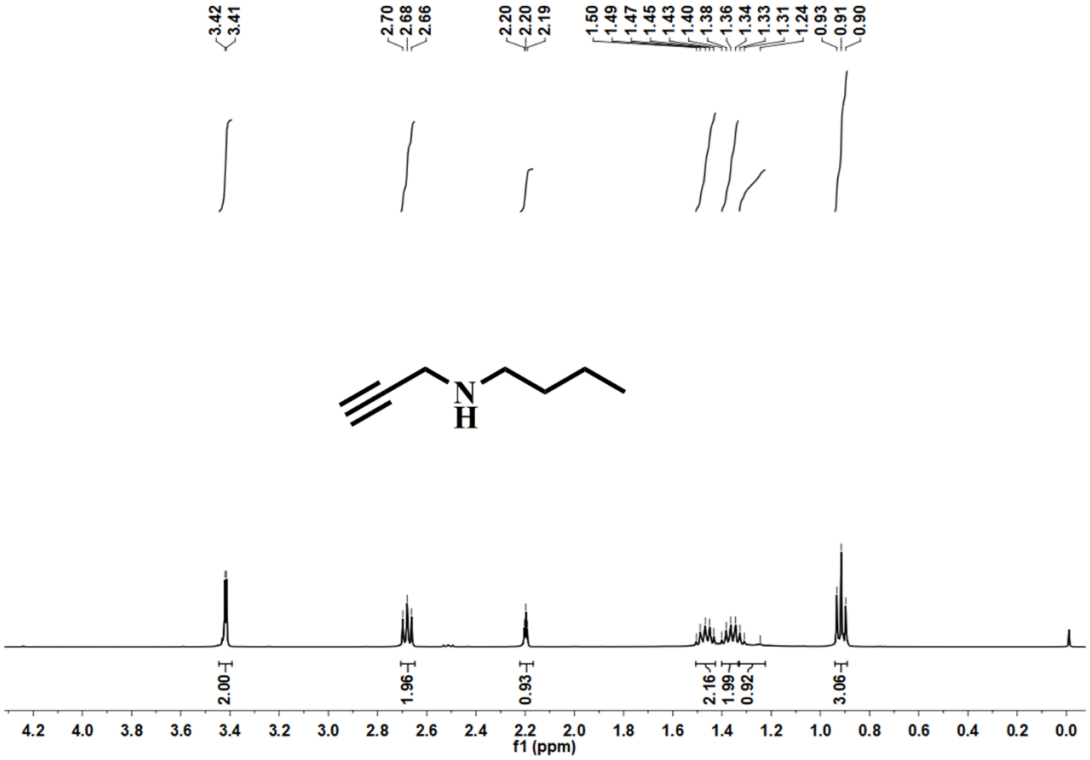

3-butyl-5-methyleneoxazolidin-2-one (2b): ^{1}H NMR (400 MHz, Chloroform-d) δ 4.75 (q, J = 2.7 Hz, 1H), 4.30 (q, J = 2.3 Hz, 1H), 4.17 (t, J = 2.4 Hz, 2H), 3.32 (t, J = 7.3 Hz, 3H), 1.60 – 1.52 (m, 2H), 1.40 – 1.32 (m, 2H), 0.96 (t, J = 7.4 Hz, 3H).

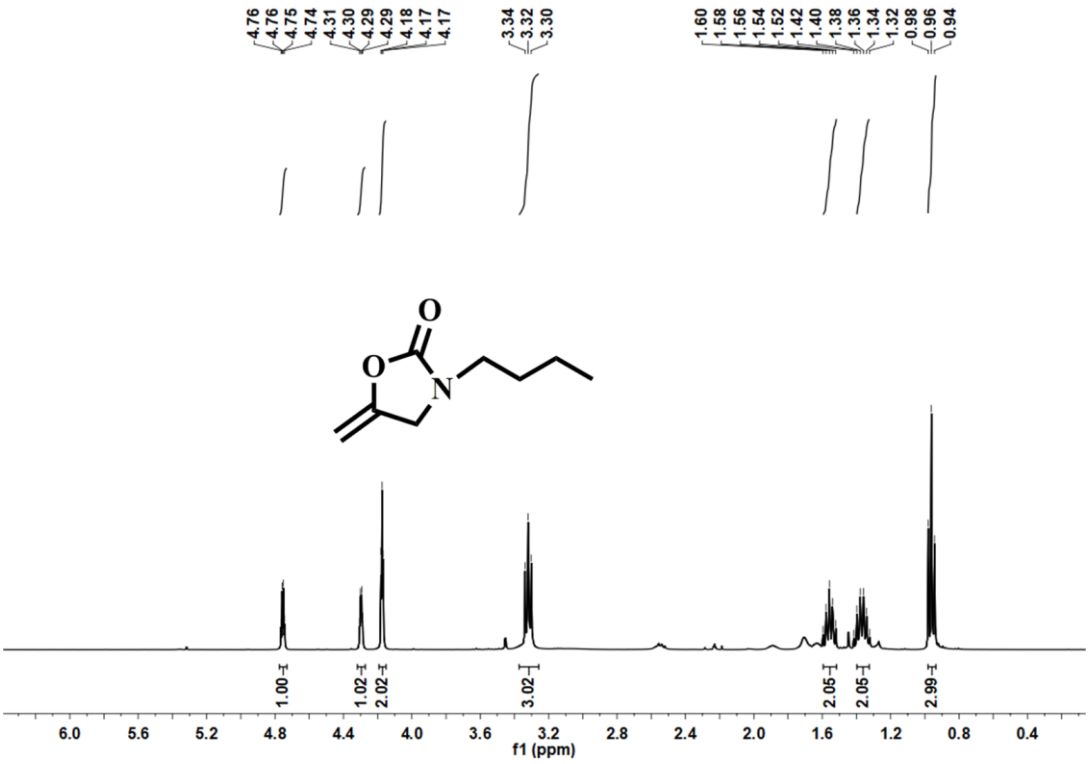

N-(cyclohexylmethyl)prop-2-yn-1-amine (3a): ^{1}H NMR (400 MHz, Chloroform-d) δ 3.43 (d, J = 2.4 Hz, 2H), 2.63 (tt, J = 10.4, 3.8 Hz, 1H), 2.17 (t, J = 2.4 Hz, 1H), 1.83 (dd, J = 12.3, 3.6 Hz, 2H), 1.71 (dt, J = 12.6, 3.6 Hz, 2H), 1.64 – 1.56 (m, 1H), 1.32 – 1.23 (m, 2H), 1.22 – 1.12 (m, 2H), 1.09 – 1.01 (m, 2H).

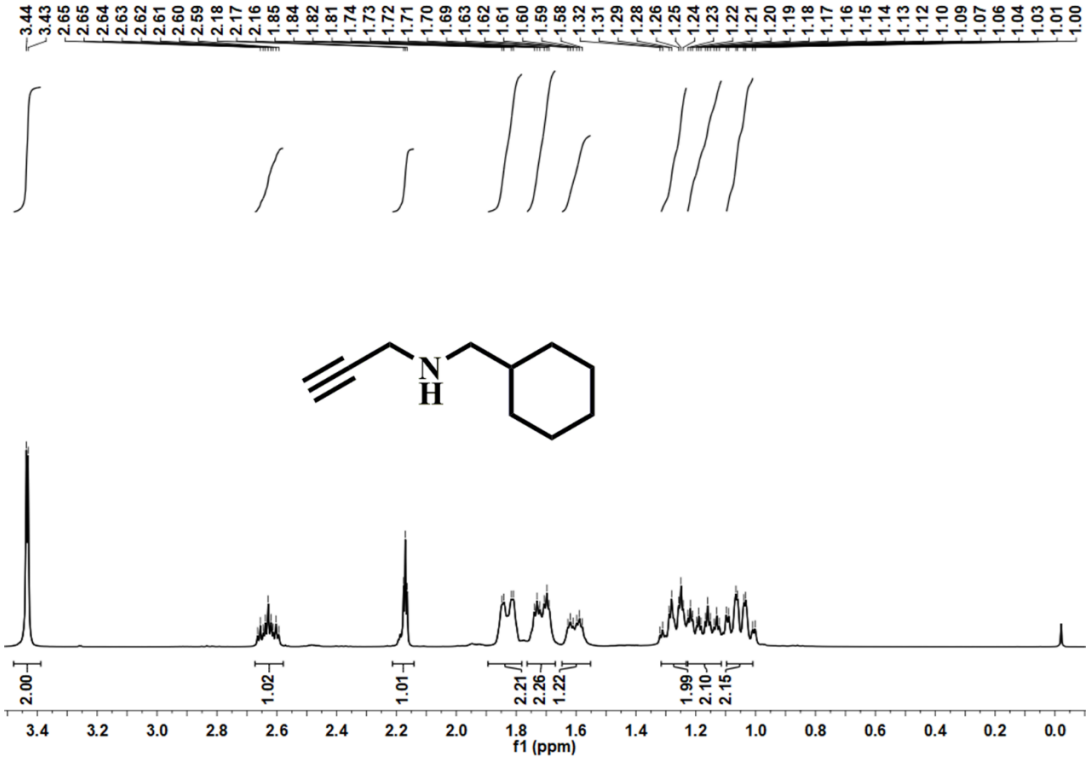

3-(cyclohexylmethyl)-5-methyleneoxazolidin-2-one (3b): ^{1}H NMR (400 MHz, Chloroform-d) δ 4.72 (d, J = 2.9 Hz, 1H), 4.26 (d, J = 2.7 Hz, 1H), 4.12 (s, 2H), 3.73 (s, 1H), 1.84 (s, 4H), 1.68 (d, J = 13.8 Hz, 1H), 1.36 (s, 4H), 1.10 (s, 1H).

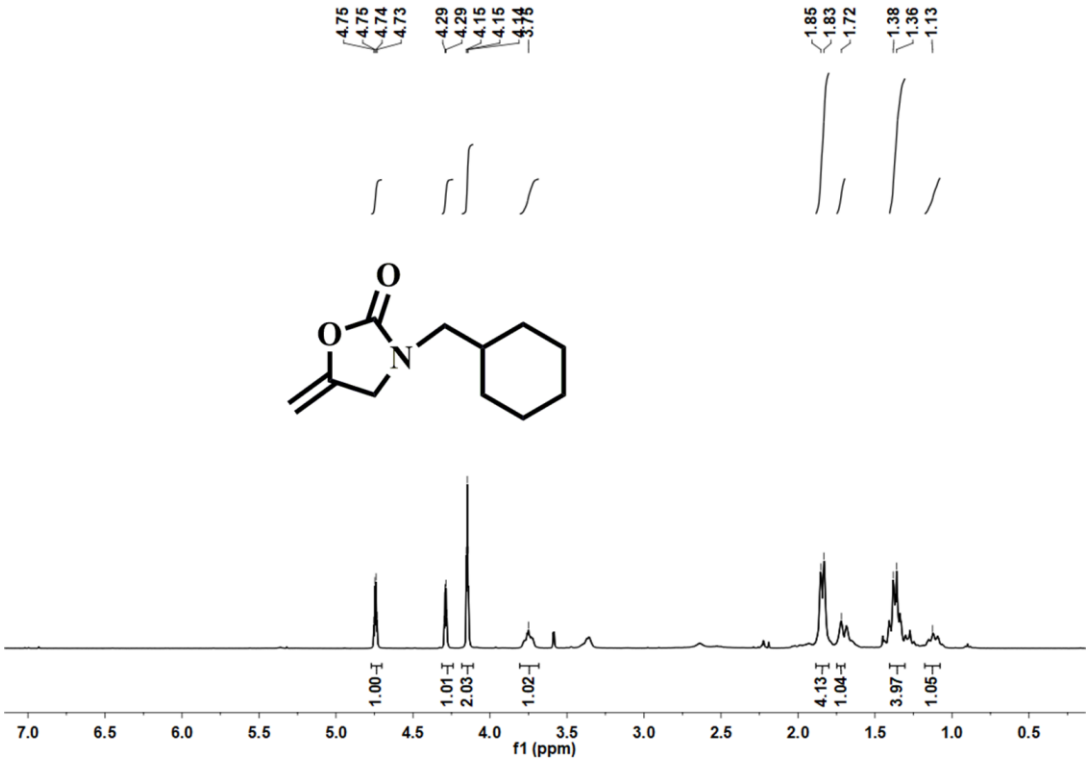

N-(thiophen-2-ylmethyl) prop-2-yn-1-amine (4a): ^{1}H NMR (400 MHz, $CDCl_3$) δ 7.25 (dd, *J* = 4.8, 1.4 Hz, 1H), 7.00 – 6.96 (m, 2H), 4.12 (s, 2H), 3.49 (s, 2H), 2.29 (t, *J* = 2.4 Hz, 1H), 1.78 (s, 1H).

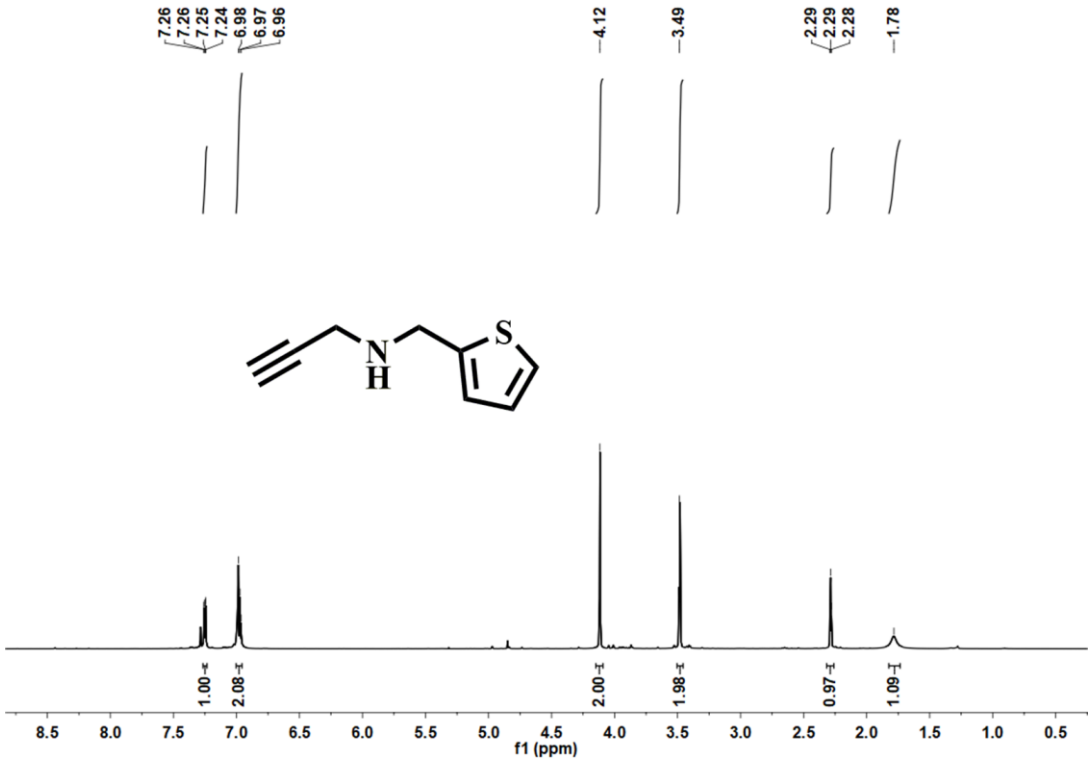

5-methylene-3-(thiophen-2-ylmethyl) oxazolidin-2-one (4b): ^{1}H NMR (400 MHz, $CDCl_3$) δ 7.30 (d, *J* = 5.1 Hz, 1H), 7.05 – 6.96 (m, 2H), 4.75 (d, *J* = 2.5 Hz, 1H), 4.67 (d, *J* = 15.0 Hz, 2H), 4.26 (t, *J* = 11.0 Hz, 1H), 4.21 – 4.03 (m, 2H).

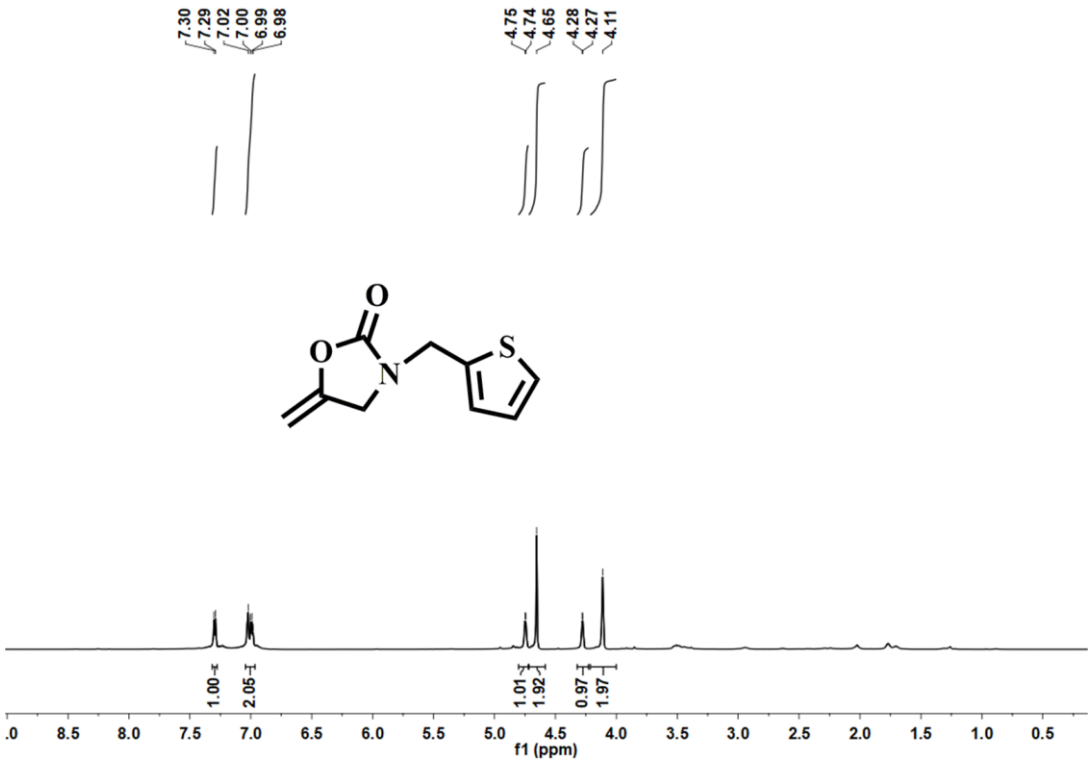

N-benzylprop-2-yn-1-amine (5a): ^{1}H NMR (400 MHz, $CDCl_3$) δ 7.41 – 7.33 (m, 5H), 3.91 (s, 2H), 3.45 (d, *J* = 2.4 Hz, 2H), 2.29 (t, *J* = 2.4 Hz, 1H), 1.77 (s, 1H).

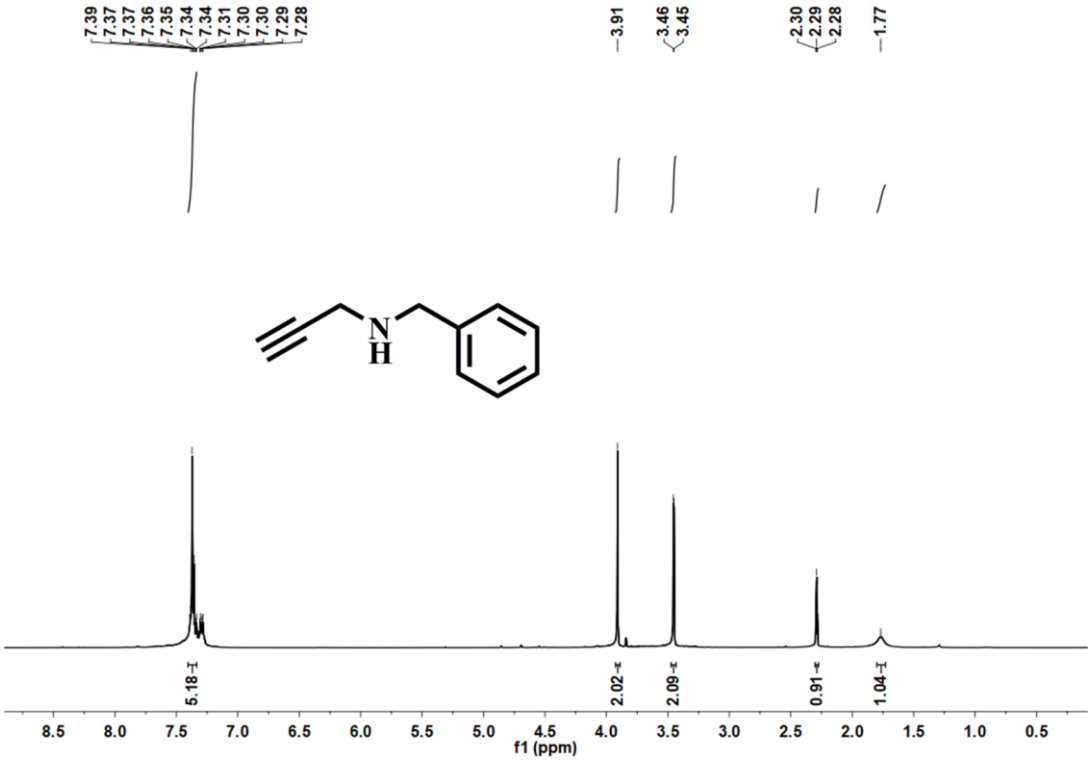

3-benzyl-5-methyleneoxazolidin-2-one (5b): ^{1}H NMR (400 MHz, Chloroform-*d*) δ 7.41 – 7.27 (m, 5H), 4.75 (dd, *J* = 5.5, 2.7 Hz, 1H), 4.48 (s, 2H), 4.26 (dd, *J* = 5.1, 2.2 Hz, 1H), 4.04 (t, *J* = 2.3 Hz, 2H).

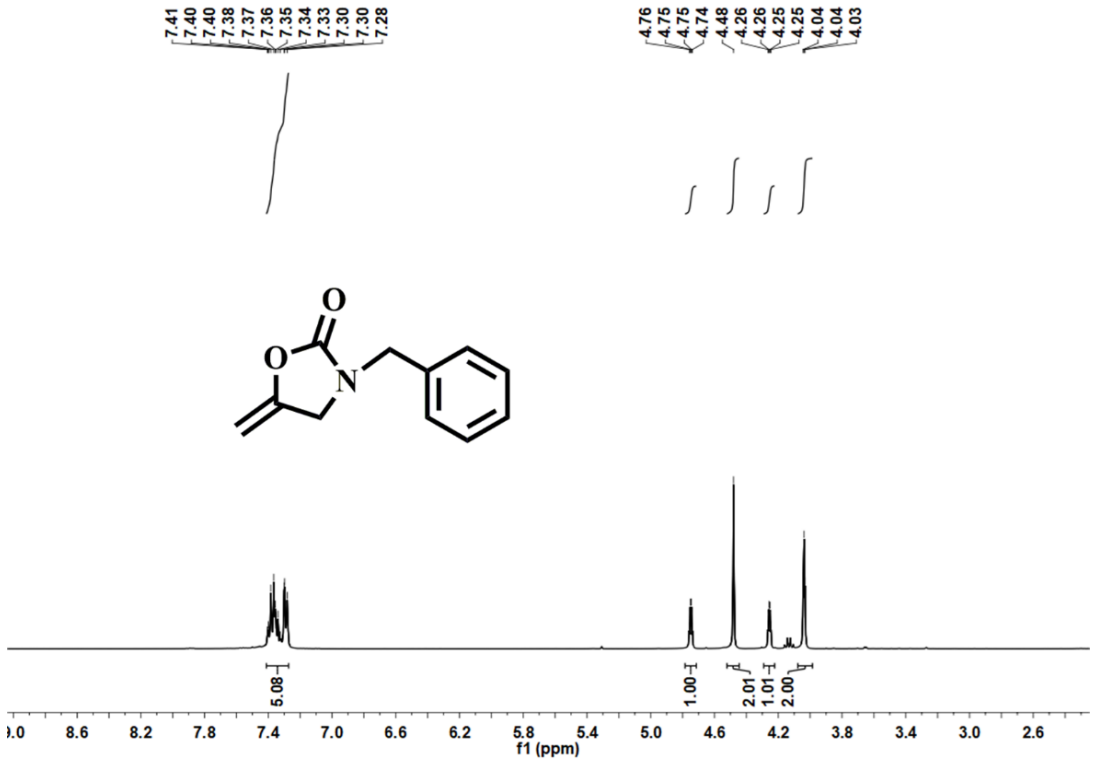

N-(4-methylbenzyl) prop-2-yn-1-amine (6a): ^{1}H NMR (400 MHz, $CDCl_3$) δ 7.63 – 7.58 (m, 4H), 7.46 (t, *J* = 8.5 Hz, 4H), 7.37 (t, *J* = 7.3 Hz, 1H), 3.96 (s, 2H), 3.49 (d, *J* = 2.4 Hz, 2H), 2.31 (t, *J* = 2.4 Hz, 1H), 1.62 (s, 1H).

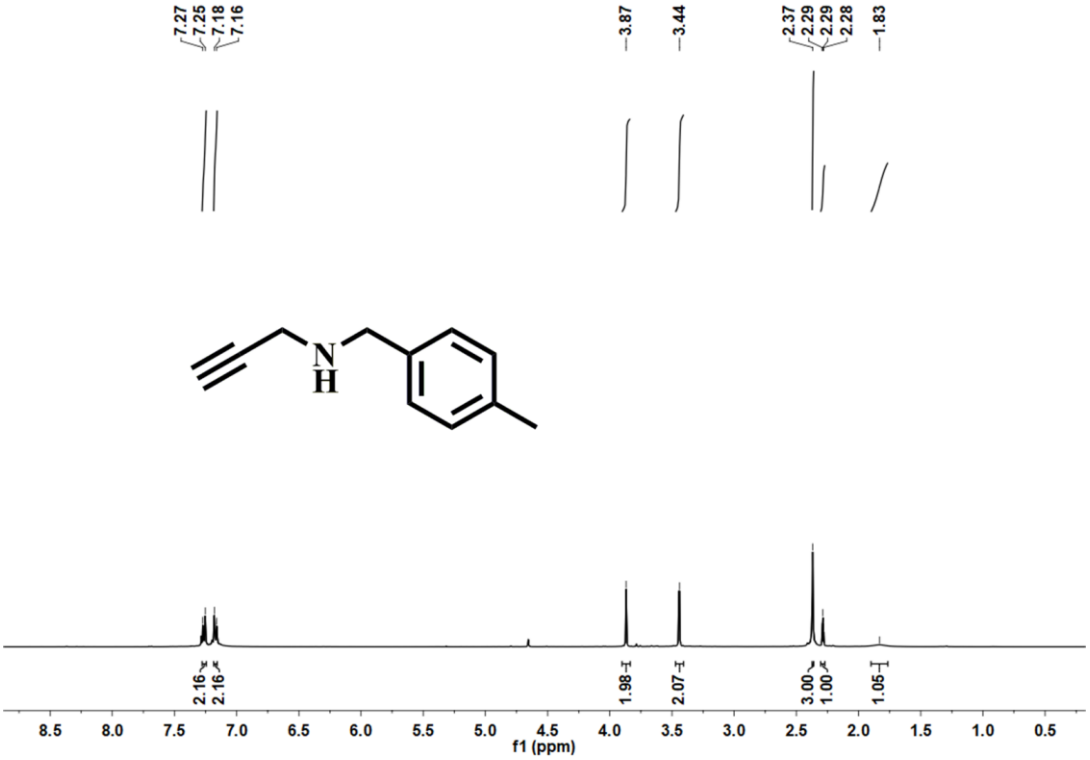

3-(4-methylbenzyl)-5-methyleneoxazolidin-2-one (6b): ^{1}H NMR (400 MHz, Chloroform-*d*) δ 7.15 (s, 4H), 4.70 (dd, *J* = 5.4, 2.6 Hz, 1H), 4.40 (s, 2H), 4.21 (dd, *J* = 4.8, 2.2 Hz, 1H), 3.99 (t, *J* = 2.3 Hz, 2H), 2.33 (s, 3H).

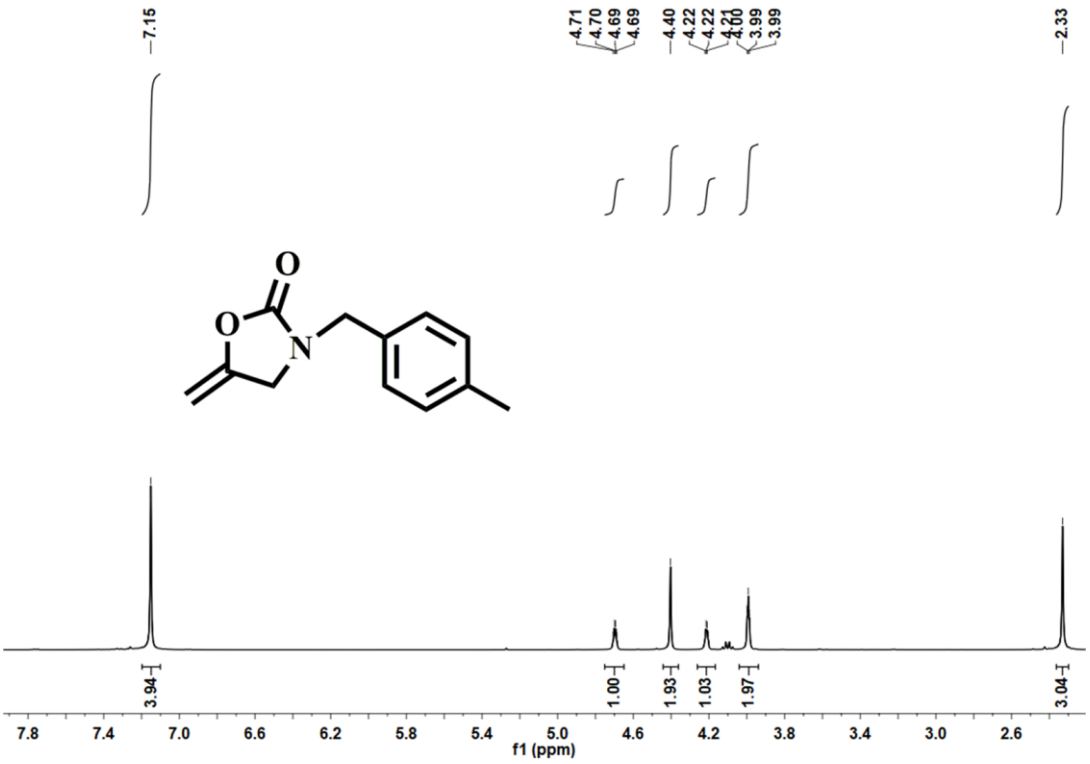

N-(4-methoxybenzyl) prop-2-yn-1-amine (7a): ^{1}H NMR (400 MHz, $CDCl_3$) δ 7.34 – 7.23 (m, 2H), 6.91 – 6.85 (m, 2H), 3.89 – 3.82 (m, 2H), 3.82 – 3.78 (m, 3H), 3.42 (d, *J* = 2.4 Hz, 1H), 2.31 – 2.24 (m, 1H).

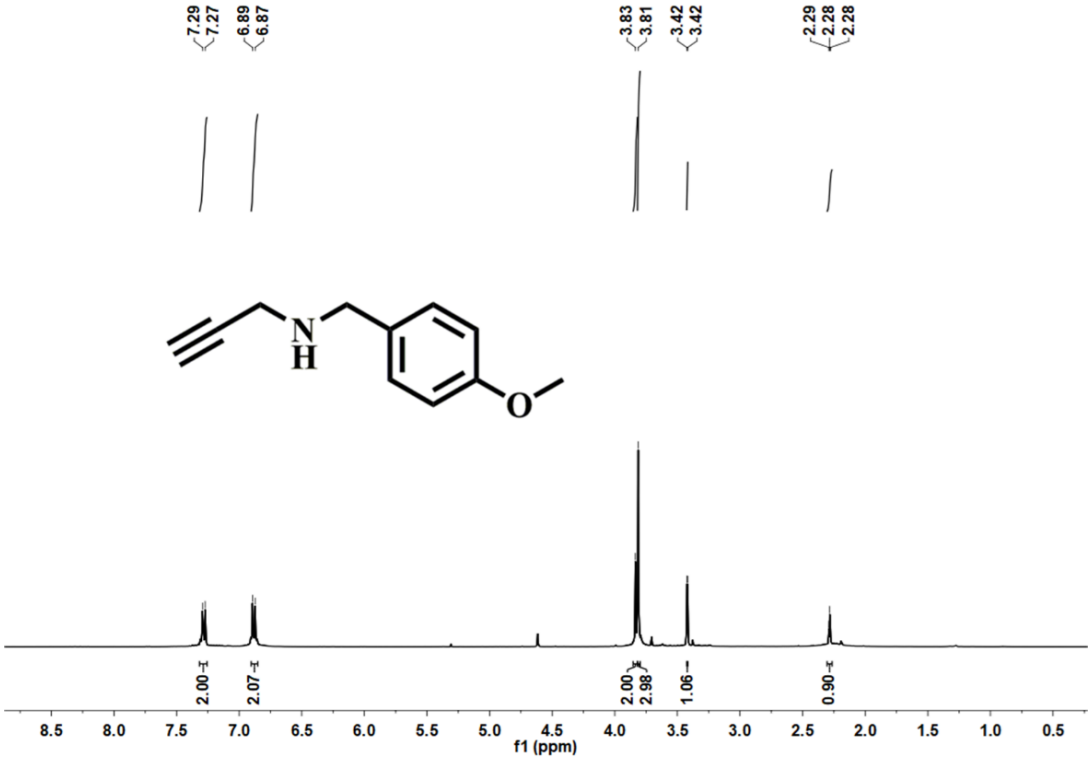

3-(4-methoxybenzyl)-5-methyleneoxazolidin-2-one (7b): ^{1}H NMR (400 MHz, $CDCl_3$) δ 7.45 – 7.09 (m, 1H), 6.89 (d, *J* = 8.4 Hz, 1H), 4.73 (s, 1H), 4.40 (s, 1H), 4.22 (s, 1H), 3.99 (s, 1H), 3.81 (s, 1H).

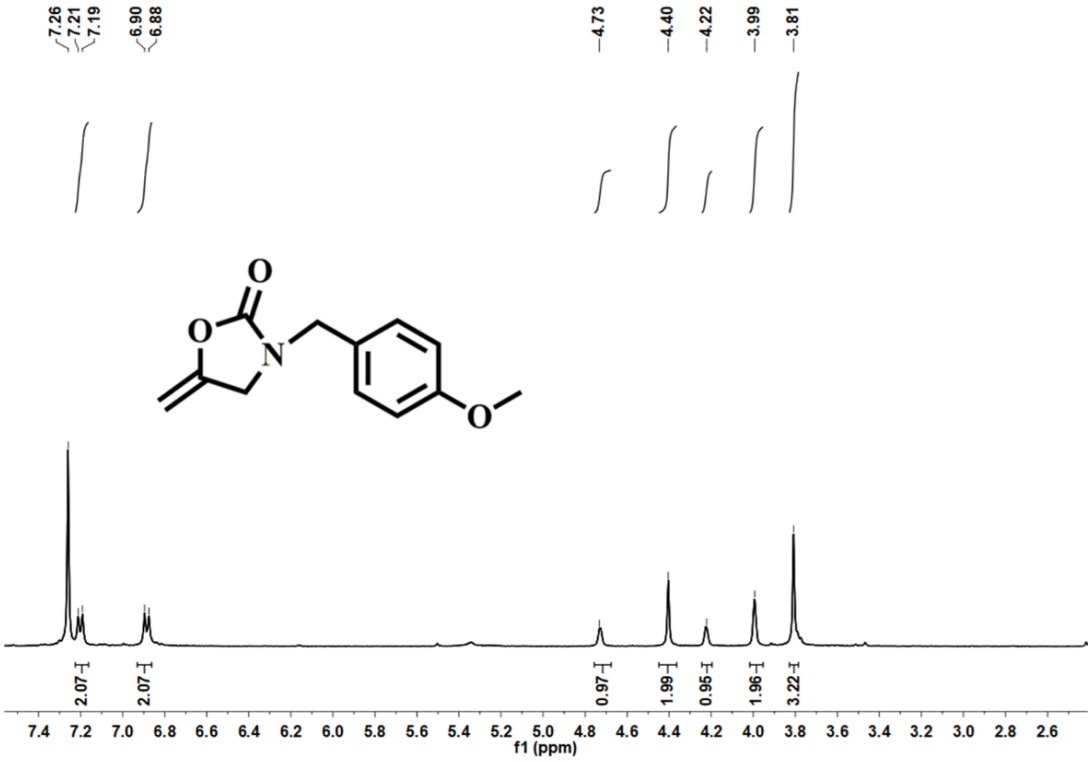

N, N-dimethyl-4-((prop-2-yn-1-ylamino) methyl) aniline (8a): ^{1}H NMR (400 MHz, Chloroform-d) δ 7.24 (d, J = 8.5 Hz, 2H), 6.74 (d, J = 8.5 Hz, 2H), 3.81 (s, 2H), 3.43 (d, J = 2.5 Hz, 2H), 2.96 (s, 6H), 2.27 (t, J = 2.4 Hz, 1H), 1.80 (s, 1H).

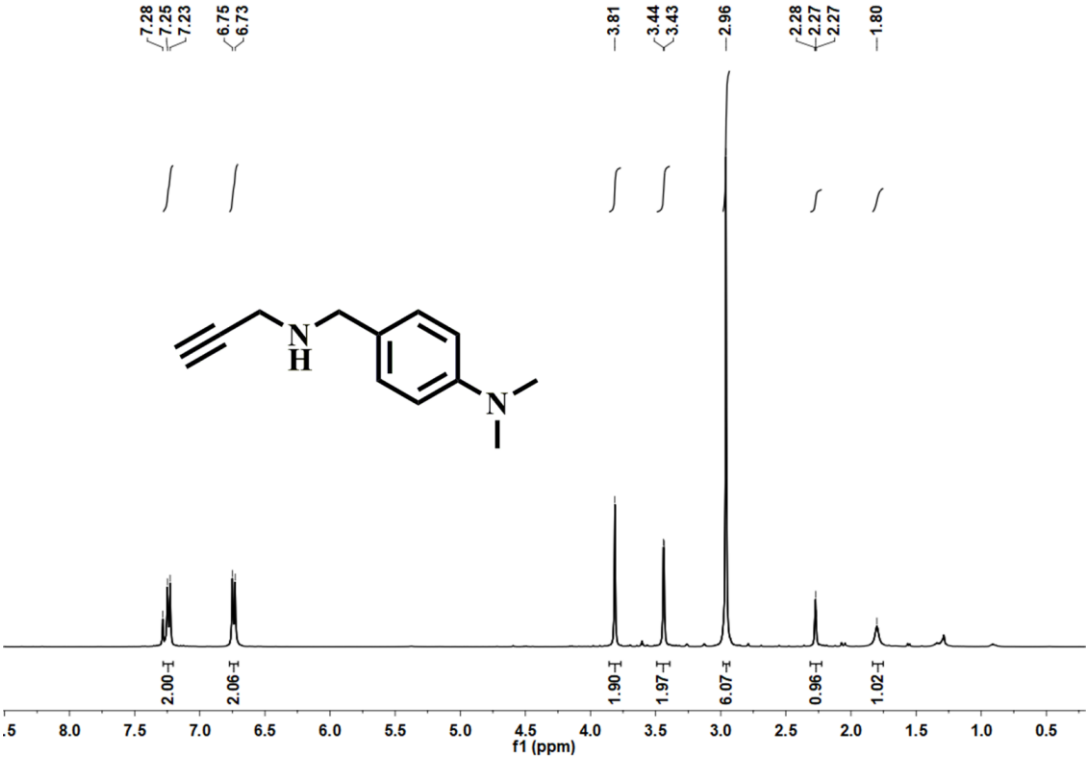

3-(4-(dimethylamino) benzyl)-5-methyleneoxazolidin-2-one (8b): ^{1}H NMR (400 MHz, Chloroform-*d*) δ 7.14 (d, *J* = 8.6 Hz, 2H), 6.69 (d, *J* = 8.6 Hz, 2H), 4.70 (dd, *J* = 5.4, 2.7 Hz, 1H), 4.36 (s, 2H), 4.20 (dd, *J* = 5.0, 2.2 Hz, 1H), 3.98 (t, *J* = 2.3 Hz, 2H), 2.95 (s, 6H).

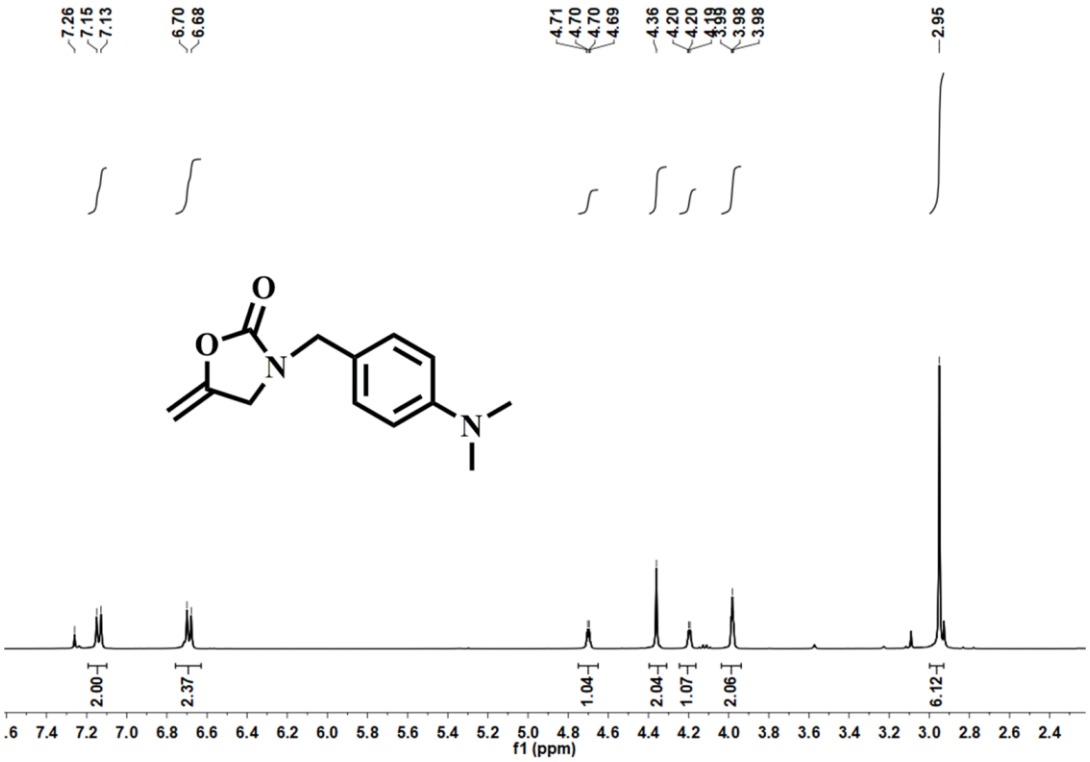

N-benzyl-2-methylbut-3-yn-2-amine (9a): ^{1}H NMR (400 MHz, Chloroform-d) δ 7.40 – 7.27 (m, 5H), 3.91 (s, 2H), 2.39 (s, 1H), 1.45 (s, 6H).

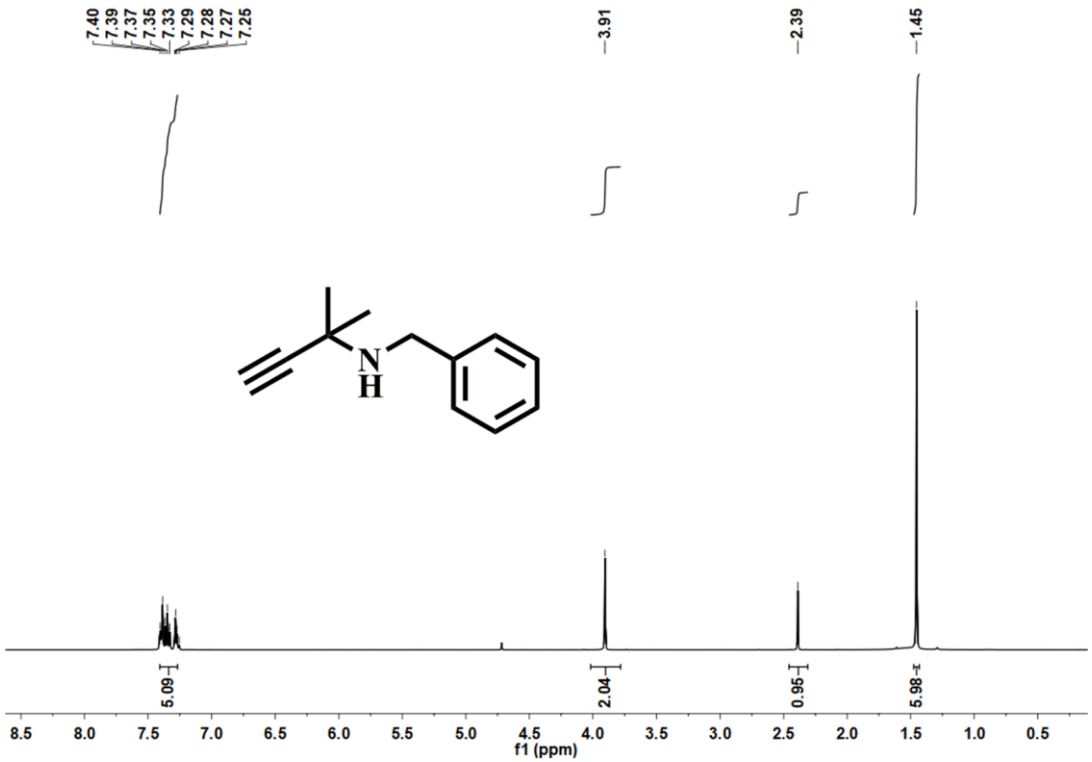

3-benzyl-4,4-dimethyl-5-methyleneoxazolidin-2-one (9b): ^{1}H NMR (400 MHz, Chloroform-d) δ 7.33 (d, J = 5.0 Hz, 5H), 4.68 (d, J = 3.4 Hz, 1H), 4.47 (s, 2H), 4.24 (d, J = 3.4 Hz, 1H), 1.32 (s, 6H).

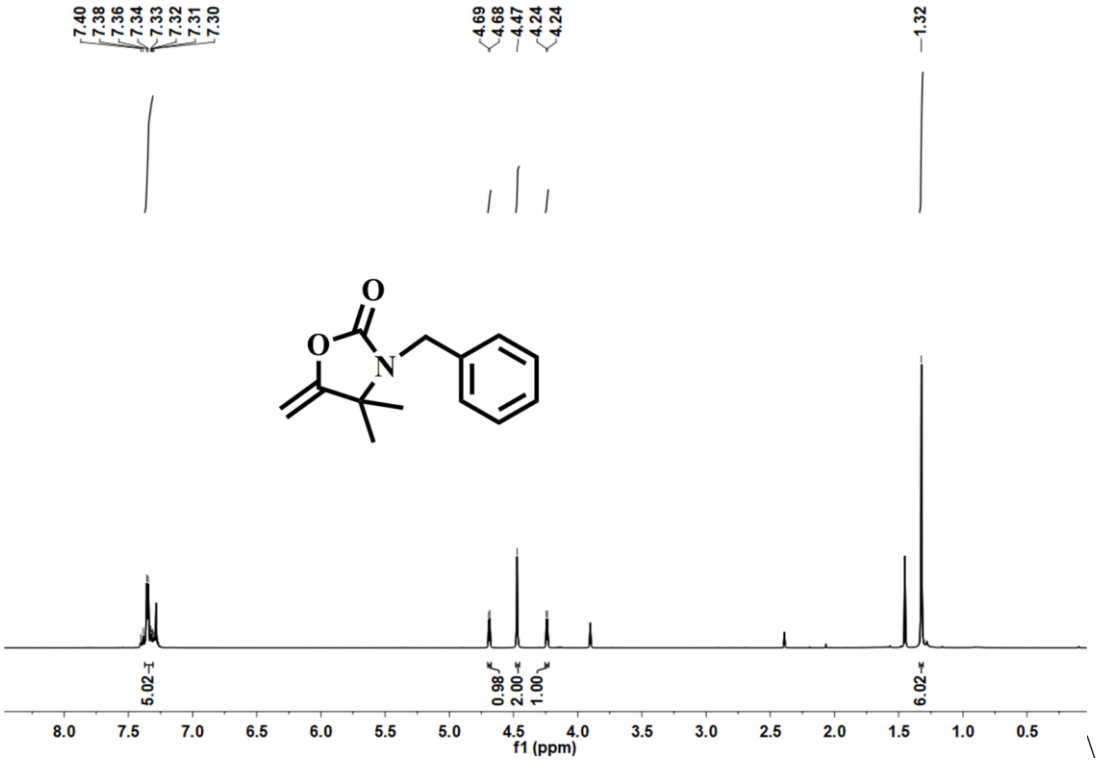

2-methyl-N-(4-nitrobenzyl) but-3-yn-2-amine (10a): ^{1}H NMR (400 MHz, Chloroform-d) δ 8.19 (d, J = 8.7 Hz, 2H), 7.57 (d, J = 8.5 Hz, 2H), 4.00 (s, 2H), 2.39 (s, 1H), 1.43 (s, 6H).

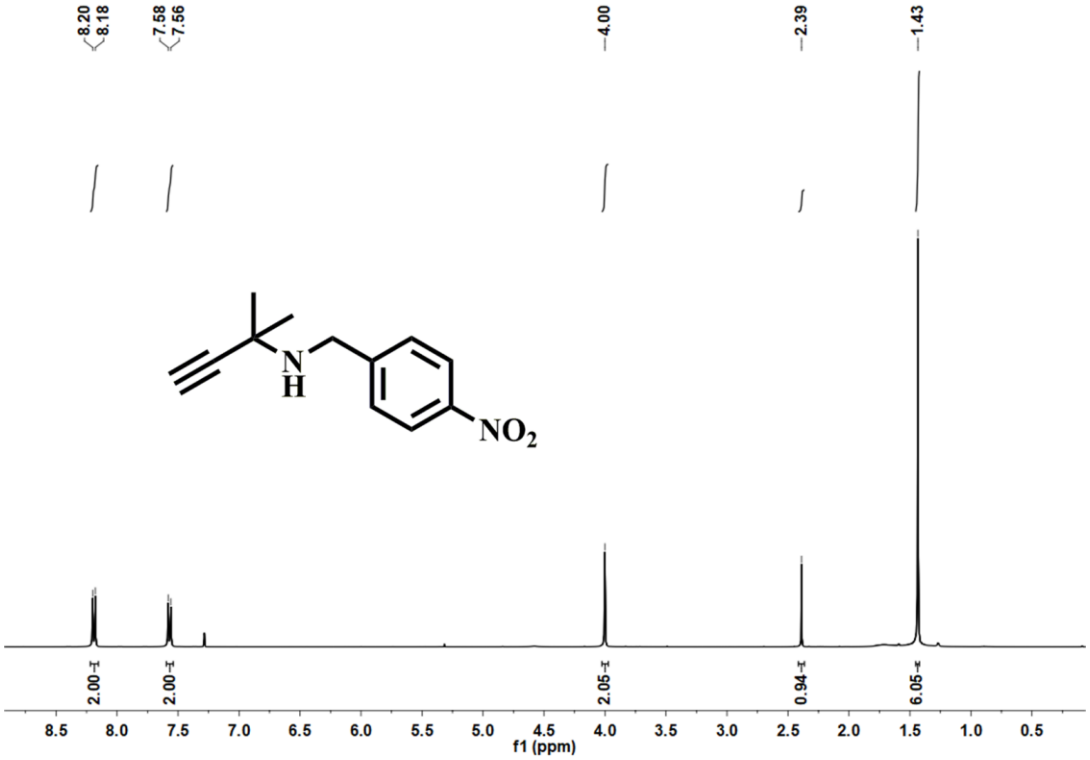

4,4-dimethyl-5-methylene-3-(4-nitrobenzyl) oxazolidin-2-one (10b): ^{1}H NMR (400 MHz, Chloroform-d) δ 8.18 (d, J = 8.7 Hz, 2H), 7.50 (d, J = 8.5 Hz, 2H), 4.71 (d, J = 3.5 Hz, 1H), 4.51(s, 2H), 4.27 (d, J = 3.5 Hz, 1H), 1.33 (s, 6H).

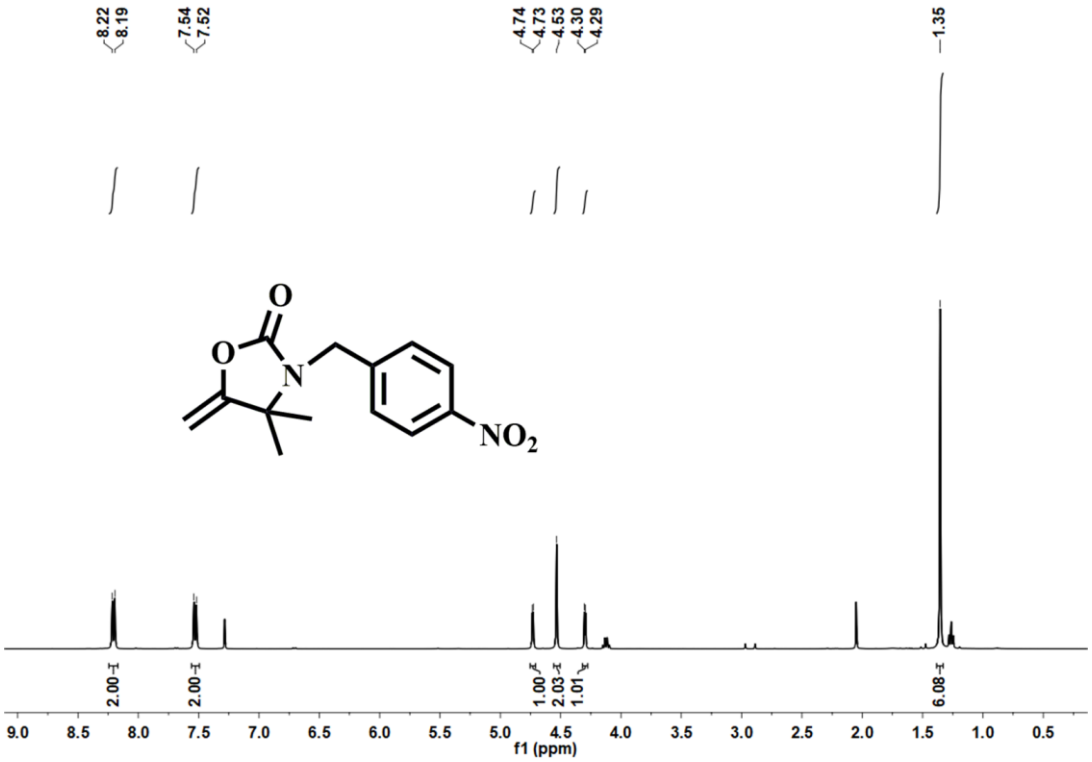

N-([1,1'-biphenyl]-4-ylmethyl) prop-2-yn-1-amine (11a): ^{1}H NMR (400 MHz, $CDCl_3$) δ 7.63 – 7.58 (m, 4H), 7.46 (t, *J* = 8.5 Hz, 4H), 7.37 (t, *J* = 7.3 Hz, 1H), 3.96 (s, 2H), 3.49 (d, *J* = 2.4 Hz, 2H), 2.31 (t, *J* = 2.4 Hz, 1H), 1.62 (s, 1H).

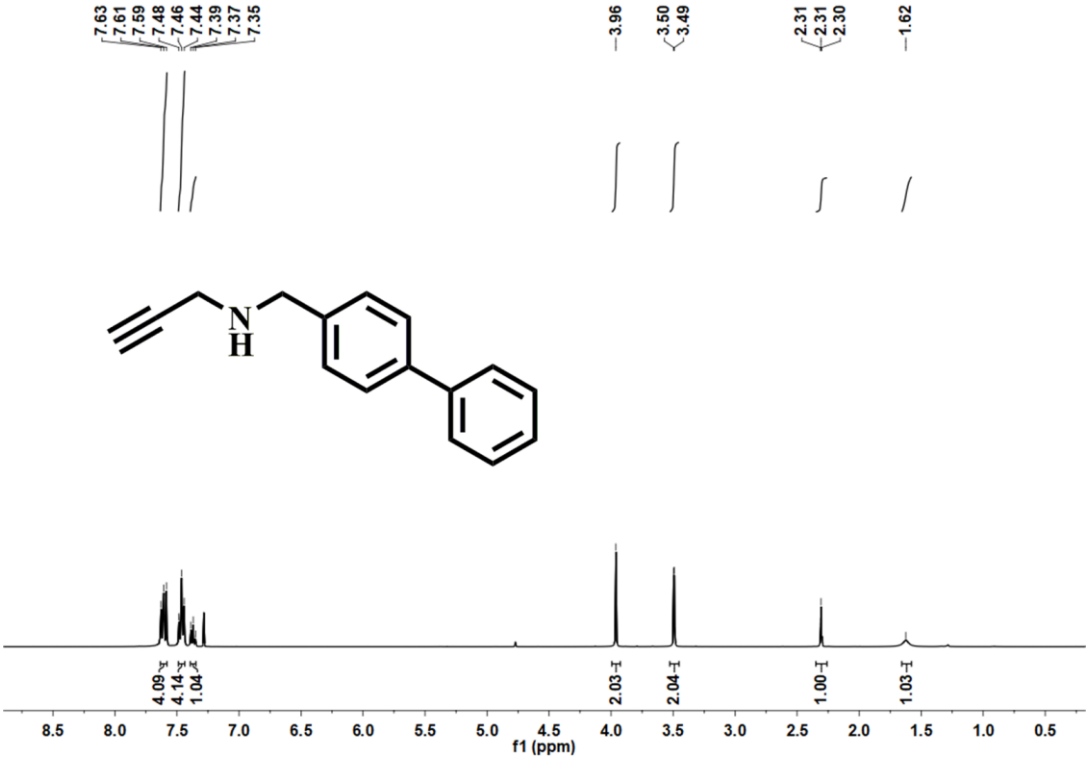

3-([1,1'-biphenyl]-4-ylmethyl)-5-methyleneoxazolidin-2-one (11b): ^{1}H NMR (400 MHz, Chloroform-*d*) δ 7.59 (dd, *J* = 7.5, 5.4 Hz, 4H), 7.45 (t, *J* = 7.5 Hz, 2H), 7.36 (t, *J* = 8.4 Hz, 3H), 4.76 (dd, *J* = 5.6, 2.7 Hz, 1H), 4.51 (s, 2H), 4.26 (dd, *J* = 5.2, 2.2 Hz, 1H), 4.07 (t, *J* = 2.3 Hz, 2H).

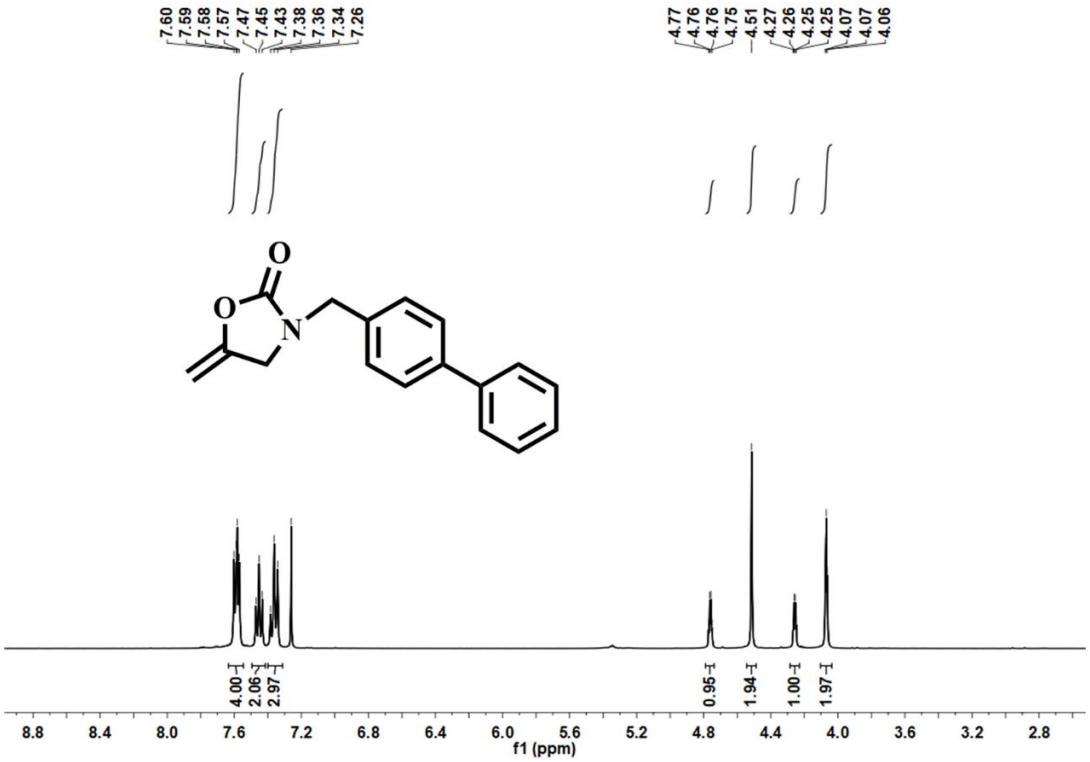

4-methyl-N-(4-((prop-2-yn-1-ylamino)methyl)phenyl)-N-(p-tolyl)aniline (12a): ^{1}H NMR (400 MHz, $CDCl_3$) δ 7.20 (d, *J* = 8.4 Hz, 2H), 7.07 (d, *J* = 8.3 Hz, 4H), 7.00 (t, *J* = 8.3 Hz, 6H), 3.83 (s, 2H), 3.47 (d, *J* = 2.4 Hz, 2H), 2.33 (s, 6H), 2.28 (s, 1H), 2.06 (d, *J* = 12.6 Hz, 1H).

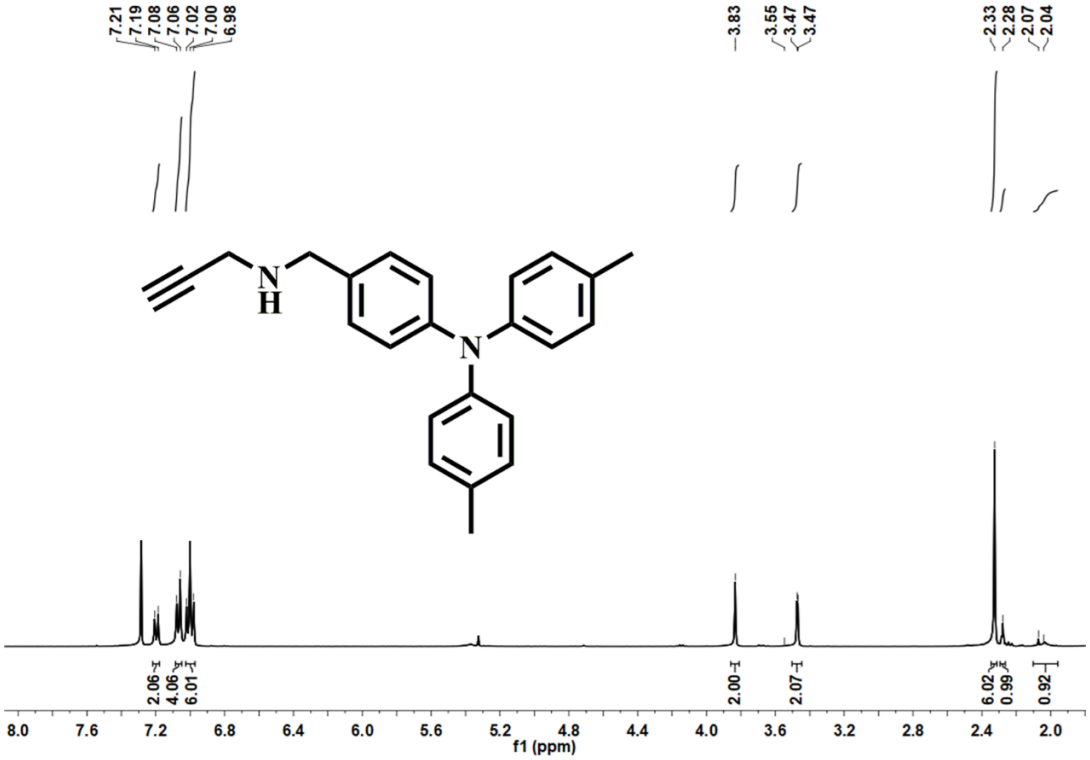

References

S1. J. Park, D. Feng, S. Yuan and H. C. Zhou, Angew. Chem. Int. Ed., 2014, 54, 430-435.

S2. J. Wang, T. Wei, Y. Liu, M. Bao, R. Feng, Y. Qian, X. Yang, L. Si and Z. Dai, Analyst., 2020, 145, 3002-3008.

S3. C.-H. Zhang, T.-D. Hu, Y.-T. Zhai, Y.-X. Zhang and Z.-L. Wu, Green Chem., 2023, 25, 1938-1947.

S4. X. Xu, Z. Li, H. Huang, X. Jing and C. Duan, Inorg. Chem. Front., 2022, 9, 3839-3844.

S5. Z. Chang, X. Jing, C. He, X. Liu and C. Duan, ACS Catal., 2018, 8, 1384-1391.